FLOW INSTABILITIES IN FLUTE-LIKE INSTRUMENTS

by
AHMED NAWAZ JANJUA

A thesis submitted to the Department of Mechanical Engineering,
Cullen College of Engineering
in partial fulfillment of the requirements for the degree of

Master of Sciences

in Mechanical Engineering

Chair of Committee: Rodolfo Ostilla-Monico

Committee Member: Kamran Alba

Committee Member: Di Yang

University of Houston
May 2020

Abstract

Flute-like instruments have a common working mechanism that consists of blowing across one end of a resonating tube to produce a jet of air that is directed at a sharp edge producing sound. Analysis of operation of flutes involves numerous research fields including fluid dynamics, physics, and aero-acoustics. In this study, an effort has been made to investigate more about the flow of air in flutes using 2D Direct Numerical Simulation. An analysis of the response of the jet of air by varying the jet width, profile, offset, and Reynolds number, and the flute labium angle in a 2D domain is the main focus of this study. We find that oscillations are sustained in the Reynolds number range 1000-2000, with lower Reynolds numbers producing no oscillations, and large Reynolds numbers developing a chaotic flow. These ranges also slightly differ for different parameters. We quantify the oscillation period and find heavy dependence on all parameters. These results lay out a framework to continue investigating instabilities in flute-like instruments.

Table of Contents

List of Tables

List of Figures

1. Introduction

1.1 Flute instruments

Flutes are considered as the oldest tunable human instruments [1] and are present in abundant cultures around the world. They are the earliest known handcrafted musical instruments. This can perhaps be attributed to their simple principle of operation; blowing across an open end of a pipe (resonator), creating a jet that is directed at a sharp edge [2].

There is an abundant variety of flutes in geometry and playing style. There are some that make soft tones like the recorders and ocarinas, whereas some are loud and noisy like shakuhachis. They all usually differ in the shape of the resonator. The resonators are generally cylindrical, but conical or spherical shaped resonators are also present.

FIG 1. 1: DIFFERENT TYPES OF FLUTE INSTRUMENTS [24]

In Fig 1.1 we have several examples of flute instruments. a) is the **recorder**. The flutist blows and the windway geometry forms the air jet, rather than leaving that to the flutist's lips. This is what makes the recorder an easy instrument to use as a beginner.

b) is the **shakuhachi**; a Japanese end-blown flute. Its end is sealed against the player's chin. This gives more flexibility in forming the air jet geometry, and thus the pitch is flexible as well. But it also is a difficult instrument to play for beginners.

c) is the **dizi** which is a Chinese transverse flute. Its distinctive feature is the thin membrane (indicated by an arrow) stretched and placed over a hole in the wall. The non-linearity of that membrane's pressure-volume curve helps transfer power from low to high harmonics, making the sound brighter and crispier.

d) are the **panpipes**. They have different resonant ducts for each note. Each duct is closed at the farther end.

e) the **ocarina** uses a Helmholtz resonator [25] to drive the jet, instead of a resonant duct. This allows it to play very low notes. For the Helmholtz resonator, the air inside the resonator acts as a spring of a certain stiffness, and the tiny lumps of air in the open tone holes act as vibrating masses on that spring.

Aside from these structural and geometric differences, there are also dynamical differences: the speeds of jets of air that enter the flutes can also vary substantially between instruments. The most significant difference, however, is in the excitation mechanism of the resonators in different flutes.

The physical modeling of flutes brings together aspects of several different domains such as physics, fluid dynamics, programming, aeroacoustics, music, and experimentation. It could lead to creating efficient flute geometries or improve existing designs, and production of rich new sounds apart from recreating sounds from existing flute designs. The optimization carried out for centuries by instrument makers and music players using their personal experience has however resulted in almost perfecting all instruments. Therefore, a very high degree of refinement has to be achieved in the physical models to come up with any meaningful suggestions on improving the instrument.

From all the types of flutes present around the world, our main focus will be on the basic recorder flute. This flute has a windway that forms the air jet which goes on to strike the edge and directs the jet in the resonator. It is a good basic test case due to its simplicity, so the recorder is the main attraction for researchers for modeling the flute instruments.

1.2 Flute geometry and sound production

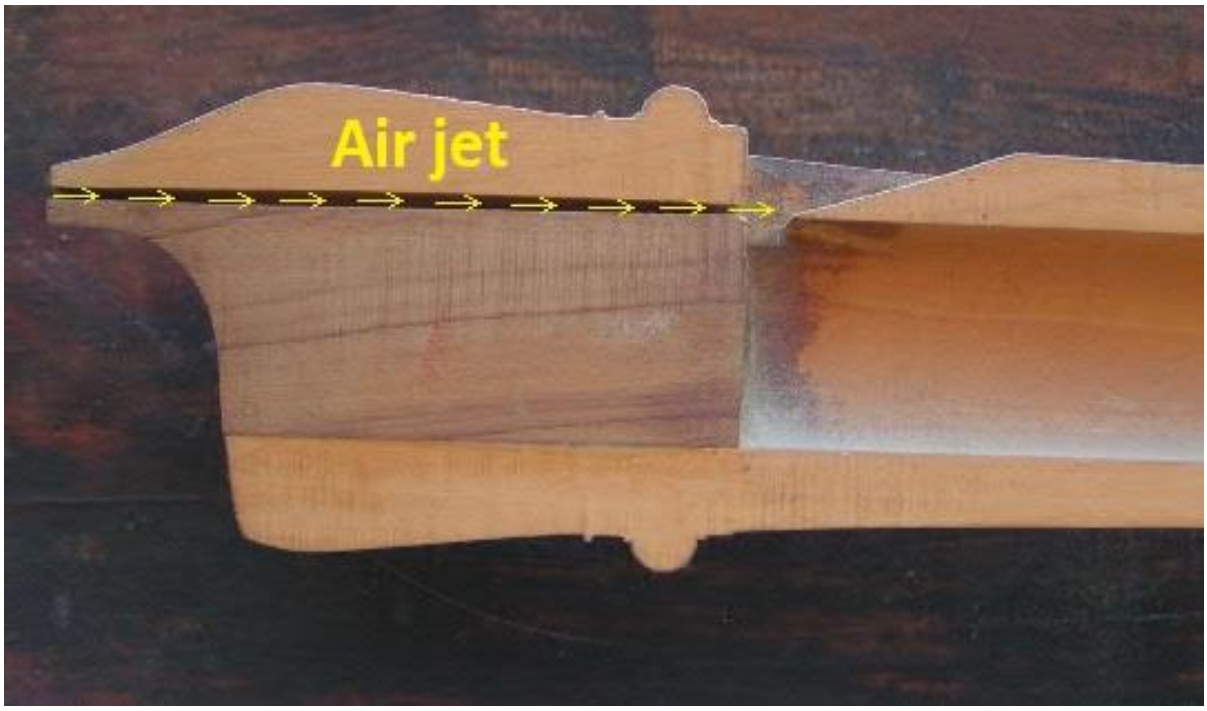

FIG 1. 2: FLUTE MOUTHPIECE [15]

Air passes through an air channel and exits to hit an edge. When it hits the edge, it does not smoothly divide into separate streams. In fact, it tends to move to one side and form a vortex. Right from exiting the flue through the slit, air is inclined to form a vortex.

The pressure created by this interaction with the edge in turn feeds back to the area of the slit where the jet is coming from, tending to push the stream upward. The opposite happens when the stream moves to the top side of the edge and then the process repeats itself. As a result, a periodic flipping of the airstream from side to side can manufacture a sound called an edge tone [3]. The continuous source of power which is needed by the air column in the flute for a sustained sound is given through the mouthpiece.

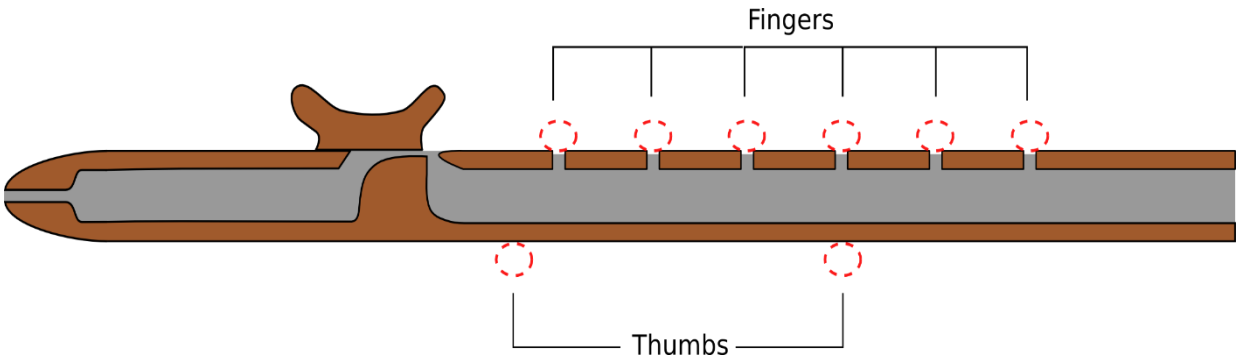

FIG 1. 3: COMPLETE FLUTE CROSS SECTION [11]

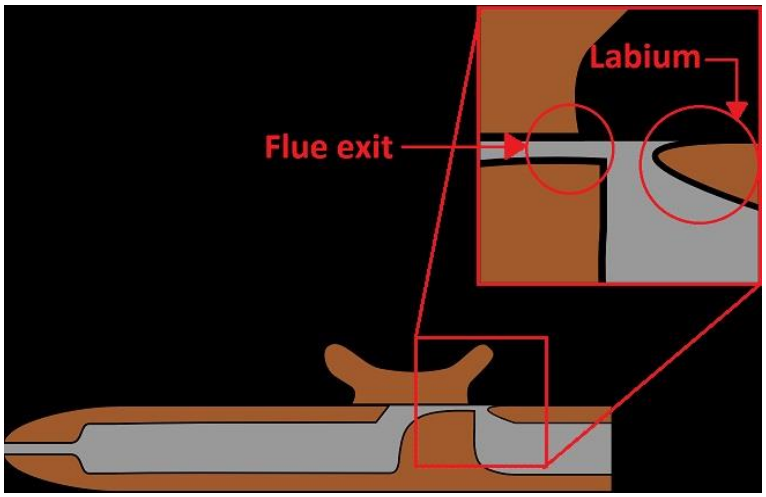

FIG 1. 4: FLUE EXIT AND LABIUM [11]

To understand how flutes make sound consider Figures 1.3-4. It shows the cross section of an average recorder flute. The flute player blows a rapid jet of air into the flute and the breath goes through the first cylinder and then into the air chamber called 'flue'. The air then exits the flue and hits the sharp splitting edge called 'labium'. When air splits going around an object, it tends to oscillate. The oscillation of the airstream above and below the labium triggers the column of air in the recorder. Very efficient tones can be manufactured by the coupling of the slit, edge, and air column (resonator).

The resonator when all the holes are closed can be thought of as an air column in an open pipe. The natural vibrations of the air in the column depend on the volume of air in it. As the ends of the air column are open at both sides, it means the pressure at these ends must be approximately atmospheric pressure. Inside the flute, the pressure need not be atmospheric and hence the first resonance occurs in the middle. Since the differential of the pressure at the ends is negligible, the ends act as the nodes. The particles inside the resonator are, however, free to move at the ends of the resonator which means that the displacement is the maximum at the ends. Therefore, the ends act as anti-nodes for displacement of the particles, with the node at the center for the first resonance.

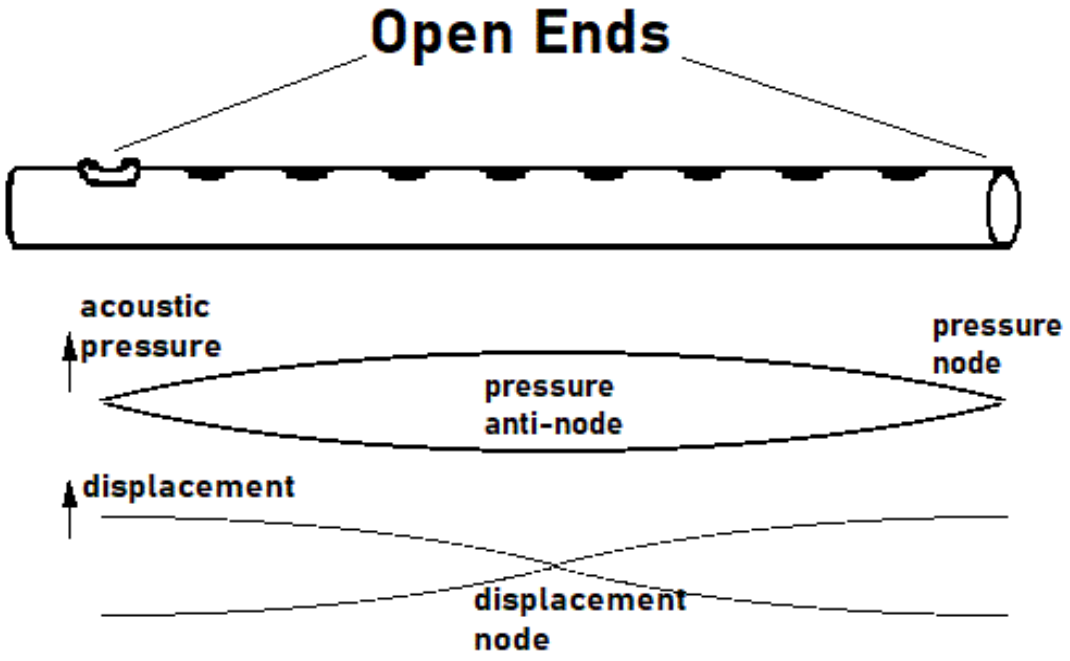

FIG 1. 5: SIMPLIFIED FLUTE RESONATOR AS AN OPEN PIPE

Figure 1.5 shows pressure and displacement in simplified flute resonator for the first fundamental frequency which occurs when all the holes are covered. The flute resonator, however, has several vibrating nodes. The air column in the resonator can be shortened by different lengths by opening holes in the resonator which change the configuration of pressure nodes, and thus the resonant frequency of this column would be different and higher notes will be observed. It can also be lengthened by closing more holes. The flautists achieve different column lengths by closing and opening or a combination of those of the six finger holes, which correspond to different resonant frequencies. This produces a variety of different ranges of sound with a very simple finger action.

As we have noticed, the role of the mouthpiece is very significant in producing edge tone and hence, vibrating the air column in the resonator. The mouthpiece excites the air in the resonator, and the continuous input of power needed to sustain oscillations to produce sound in a flute is given to the recorder by the mouthpiece. So, in our study our main focus is the flow of air in the mouthpiece as it leaves the flue and hits the labium edge to produce an edge tone.

1.3 Basic Operation

Instruments from the flute family all have a similar principle of operation. An unstable jet of air comes out from either a flow channel and is directed towards the labium. Air jets are inherently unstable, therefore this perturbation travels and gets amplified spontaneously along the jet. The interaction of the unstable flow with the

labium provides the necessary acoustic energy to sustain the acoustic oscillation in the resonator.

The sound produced when air is split and starts to oscillate around the labium edge is called edge tone. At the surface of the labium, as the boundary layer thickens, and flow becomes more unstable. The velocity profile also evolves as the jet moves forward and the air particles outside the jet interact and become a part of jet smoothing. The jet creates a vortex which evolves and interacts with the incoming incident jet itself. This in turns gives rise to oscillations of the jet around the edge of the labium.

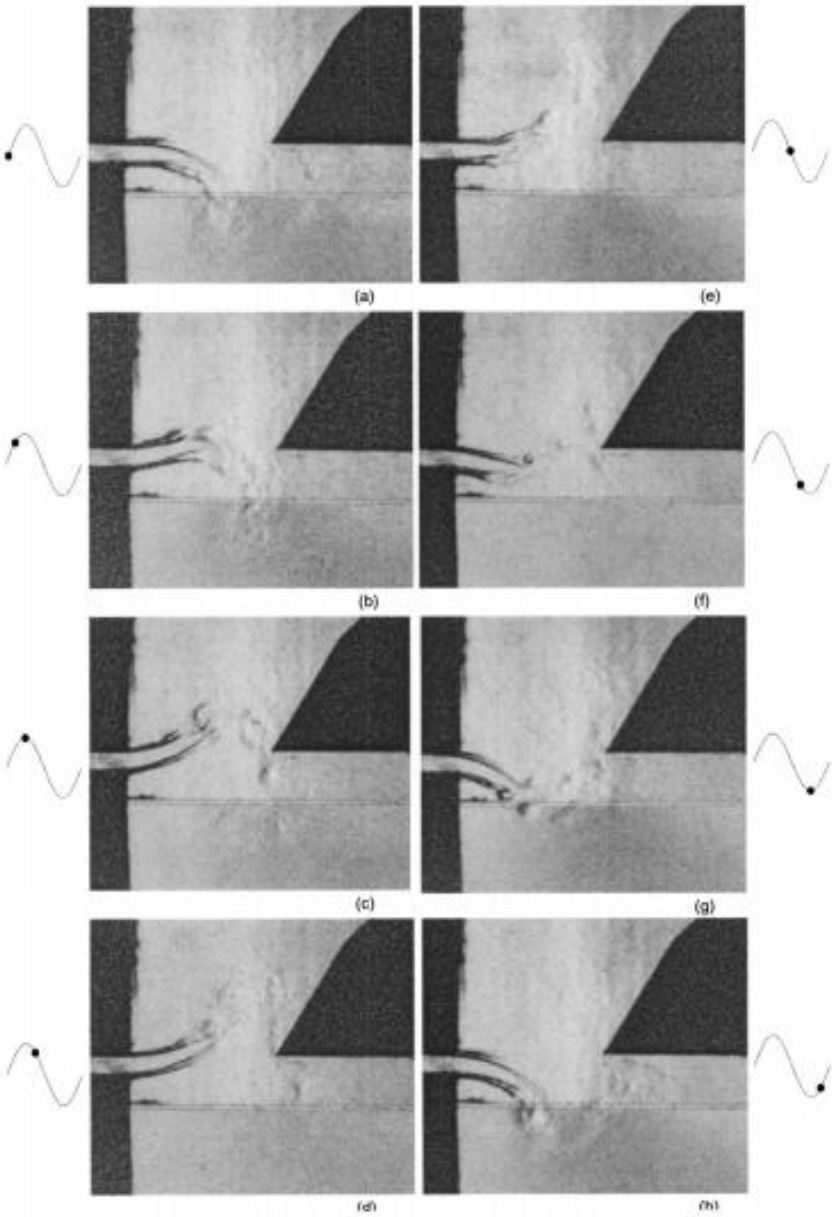

FIG 1. 6: TIME SEQUENCE OF VORTEX SHEDDING AT 60-DEGREE LABIUM. JET SWINGS AROUND THE LABIUM INTO AND OUT OF THE FLUTE RESONATOR [16]

When the air jet is directed at the flute labium and the flow grazes the inclined labium surface, it goes through a change in its initial velocity profile. Because of the geometry of the labium, the jet gets constricted and faces a favorable pressure gradient which tends to accelerate the flow. Due to viscous forces near the labium, fluid elements tend to stick to the surface of the labium, and this imposes

the no slip condition on the surfaces. This faint favorable pressure and fluid viscosity try to keep the flow stuck to the surface of the labium on its inclined side until the perturbation exceeds the effects of this favorable pressure.

With changing parameters, the sound produced also changes as evident by the change of pressure of air and tone of sound. We will discuss how changing different parameters affects this oscillatory motion of the fluid around the labium using computational methods.

1.4 Background

The first published studies of instruments like flutes were perhaps from Bernoulli [4] and Mersenne [5]. They consist mainly of analyses of the air column (resonator) resonance frequencies. It is very useful in understanding several construction properties of the resonator: position, shape corrections, diameter of tone holes etc.

For modeling the source mechanism, Helmholtz [6] and Rayleigh [7] were the first one to propose such models. According to Helmholtz, it could be a flow source, just periodically injecting a volume inside a resonator, hence the working could be described as a monopole. Whereas, Rayleigh persisted that because the sources act as the open end of the bore, they are more appropriately described as a dipole. Close to the open ends of the bore, the velocity fluctuations are large, but the pressure fluctuations are very small, which supported the reasoning that the source acted as one end of a dipole. In the comments of the second version of his book, Helmholtz made it clear that he changed his opinion on the source model being a

monopole. These observations laid the basis for further modeling of source mechanism e.g. as described by Verge in [17] with a jet-drive model and Holger in [22] with a discrete vortex model which will be discussed in next sections.

In the beginning of the sixties, the works by Powell [8] suggested a feedback loop model on the type of tone produced when the jet hits an edge only, with no resonator placed ahead. This type of tone is called an edge tone. However, the actual amplitude of the oscillation can only be predicted by a non-linear model by Fletcher [9]. This approach has inspired many other descriptions based on loop systems.

More models continued to be developed in the next decade, but they did not completely suit flute instruments. But a very rigorous approach taking aero-acoustics and fluid mechanics into account was followed by Howe [10]. Other groups also joined in adopting an intermediate approach inspired by the works of Powell [8], Fletcher [9], Coltman [12,13] using simplified description and rigorous formulation, producing sound though models that use lumped elements with principles of aero-acoustics.

1.5 Current models used and their limitations

Currently, the research on modeling the flute instruments is basically classified in two distinct groups. First is the approach that uses lumped elements which divide the flute into independent blocks that can be individually analyzed and then the blocks with known behavior are attached back together to reconstruct the original setting. These lumped models are discussed in detail in [14]. The lumped-element feedback models established by Cremer and Ising [30] in 1967 still serve as

the dominant paradigm in understanding flute-like instruments for more than 50 years. There have been modern versions proposed for these models. Lumped models are usually linear and break down the original problem into easily solvable smaller parts and the whole problem is approximated in a simple and piecemeal manner. So, it sacrifices the intricacies and rigor that should be involved. An advantage of them is that they can be used to model different instruments by interchanging pieces separately instead of as a whole.

The second approach uses Integration techniques as used by Howe [10], Elder [27], Crighton [28] and Bechert [29] that are more rigorous than lumped-element models and ideally would produce more realistic results, but at the same time they are also very mathematically complex. These models describe the flow and acoustic field interaction using integral methods with mathematics that is only valid for a few types of geometries that are idealized. These models also use some hypotheses like vortices being punctual, and infinitely thin shear layers which are restrictive, and make these models less suitable for real-time implementations.

Theories have been proposed that relate the ratio of the distance from the flue exit to the labium and jet width, with the velocity of the acoustic perturbation caused by the jet in [18] and [16]. The most difficult part of modeling the flutes at the moment is the behavior of the jet under acoustic excitation. So, another model is also needed to describe the formation of the jet as it attacks, before it reaches the flute labium. A model is proposed for that in [17].

There are a few other conveniences too when applying these models to flute-like instruments. These models are based on linear perturbations and are hence applicable only to small transverse jet oscillations. Looking at flow visualizations for different geometries of flutes [18] shows that transverse oscillations of the jet can even reach amplitudes greater than the flue channel height. So, they are only valid for short distances, since the flow tends to roll up into discrete vortices further downstream. Finally, the viscosity is normally neglected in the models. So downstream from the flue exit, these models assume a constant velocity profile for the jet. This assumption is only valid for low Reynolds numbers i.e negligible boundary layer. Whereas most of the instruments in the flute family work at Reynolds numbers (defined in section 2) above 1000, which means that jet would have a smooth initial velocity profile.

As it becomes clear from the discussion above, the models are incomplete and of limited applicability. To form better models, a better understanding of what is going in the different parts of the flute is needed. This comes with detailed experiments and simulations which do not start with apriori models. For this thesis, we focus on a particular part of the flute, and study it with numerical simulations. The aerodynamics of the incoming jet around flute labium is studied by simulating it using Direct Numerical Simulation (DNS) based on the Navier-Stokes equations in two dimensions. Spatial maps for velocity for the entire domain are simulated for a significant number of timesteps giving us access to complete velocity data, and a detailed picture of vortex shedding that occurs around the labium.

Thus, we aim to generate the results needed to validate the current models or even improve them. As we will have the velocity data for the entire domain, we will be able to provide more detailed information than experiments. Changes in the velocity maps as a result of variation in certain parameters are also observed and investigated.

2. Simulation Details

2.1 Governing Equations

In the Eulerian framework, the components of the velocity at any point (*x*,*y*,*z*) are denoted as *u*, *v*,and *w*. The velocity components are unknowns that depend on the independent variables *x*, *y*, *z*, and *t* where *t* is time. The description of the motion for any value of *t* at any point in space is:

$$u = u(x, y, z, t), v = v(x, y, z, t), w = w(x, y, z, t)$$

The basic governing equations are the incompressible Navier-Stokes equations that solve for pressure and velocity fields at each timestep.

The equation for conservation of mass is written as

$$\frac{\partial \rho}{\partial t} + \nabla \cdot (\rho \vec{V}) = 0 \quad , \tag{1}$$

where ρ is density, *V* is the velocity vector and ∇ is gradient operator.

Because of incompressibility, the density of the fluid does not change with time, so the equation becomes

$$\frac{\partial \rho}{\partial t} = 0 \longrightarrow \nabla \cdot \vec{V} = \frac{\partial u}{\partial x} + \frac{\partial v}{\partial y} + \frac{\partial w}{\partial z} = 0 \quad . \tag{2}$$

Using the law of conservation of momentum in each dimension, Navier-Stokes equations can be written as

$$\rho\left(\frac{\partial u}{\partial t}+u\frac{\partial u}{\partial x}+v\frac{\partial u}{\partial y}+w\frac{\partial u}{\partial z}\right)=\rho g_x-\frac{\partial p}{\partial x}+\mu\left(\frac{\partial^2 u}{\partial x^2}+\frac{\partial^2 u}{\partial y^2}+\frac{\partial^2 u}{\partial z^2}\right) \quad , \quad (3)$$

$$\rho\left(\frac{\partial v}{\partial t}+u\frac{\partial v}{\partial x}+v\frac{\partial v}{\partial y}+w\frac{\partial v}{\partial z}\right)=\rho g_y-\frac{\partial p}{\partial y}+\mu\left(\frac{\partial^2 v}{\partial x^2}+\frac{\partial^2 v}{\partial y^2}+\frac{\partial^2 v}{\partial z^2}\right) \quad , \quad (4)$$

and $$\rho\left(\frac{\partial w}{\partial t}+u\frac{\partial w}{\partial x}+v\frac{\partial w}{\partial y}+w\frac{\partial w}{\partial z}\right)=\rho g_z-\frac{\partial p}{\partial z}+\mu\left(\frac{\partial^2 w}{\partial x^2}+\frac{\partial^2 w}{\partial y^2}+\frac{\partial^2 w}{\partial z^2}\right) \quad . \quad (5)$$

'g' in these equations stands for gravitational acceleration in the direction of the respective subscript. For this problem, there is no thermal interaction involved, so the energy equation is not needed.

Through a characteristic length *L*, and a characteristic flow velocity *U*, we non-dimensionalize the equations using the following scales:

Non-dimensionalized velocity u* = u / U,

Non-dimensionalized length r* = r / L,

Non-dimensionalized time t* = t / (L/U),

Non-dimensionalized pressure p* = p / (ρU^2),

We choose as characteristic length the domain-size, and as characteristic speed a jet velocity. Hence, the domain size and the jet velocity become one in these non-dimensional scales. This also gives us the definition of the Reynolds number (Re) as Re = UL /nu , where nu is Kinematic viscosity.

The time advancement of equations 3-5 uses fractional step methods as described in [19] and [23], which show that inconsistencies can arise in solution if

velocity boundary conditions are used for the calculation of the immediate velocity fields. Since the continuity term does not contain the time derivative term explicitly, this gives a major difficulty in getting accurate solutions. Implicit coupling is done between the continuity equation and the pressure in momentum equations to achieve the constraint. Numerical instability can also arise if the scheme fails to preserve the global conservation of the quantities like momentum, circulation, and kinetic energy.

Conservative forms of non-linear terms are used to minimize truncation errors associated with second order finite differencing methods that need to be taken care of and are more pronounced near the wall. Fractional time-stepping is carried out using a third-order low storage Runge-Kutta method for the convective term, and a second-order Crank-Nicolson Implicit scheme for the viscous term. The implicit method for viscous terms eliminates the numerical stability restriction.

2.2 Numerical Setup

The problem is simulated using Direct Numerical Simulations of the incompressible Navier-Stokes equations. No turbulence models are used here. Because the geometry of the domain of interest is structured and simple shaped, we have used Cartesian coordinates for the time dependent simulations in two dimensions. Instabilities in three dimensions are not simulated so it is hard for us to comment on what order of accuracy these two-dimensional simulations are compared to the real air flow in flutes.

Spatial discretization of the domain is done using the Finite-Difference Method (FDM). There are however efficient spectral methods in any coordinate system that are more accurate than the FDM. But FDM also has some inherent advantage over other methods. FDM efficiently takes care of geometric constraints and is more flexible for boundary conditions especially when global conservation properties are maintained. As shown by Rai *et al.* [19] and Choi *et al.* [20], second order FDM schemes are sufficient to describe lower order turbulence statistics.

The domain is multiple lengths longer in the direction perpendicular to the jet than the direction parallel to the jet. This is done to make the effects of the sidewalls as negligible as possible. The domain is discretized into a certain number of points in y-direction (perpendicular to the jet) and z-direction(parallel to the jet) respectively for lower Reynolds numbers and as the Reynolds number is increased, the resolution is also increased to capture the flow dynamics correctly.

In particular, the resolution is increased from 384x128 points (Figure 2.1) for the lower Reynolds number cases to 768x256 (Figure 2.2) for the higher Reynolds number cases in the y and z-directions respectively. And the number of grid points inside the jet when the jet width is 0.1L is 13. This is done not only to account for the increasing domain size, but also for the smaller-scale structures appearing in the flow. The resolution is increased when dispersive errors in the vorticity become apparent.

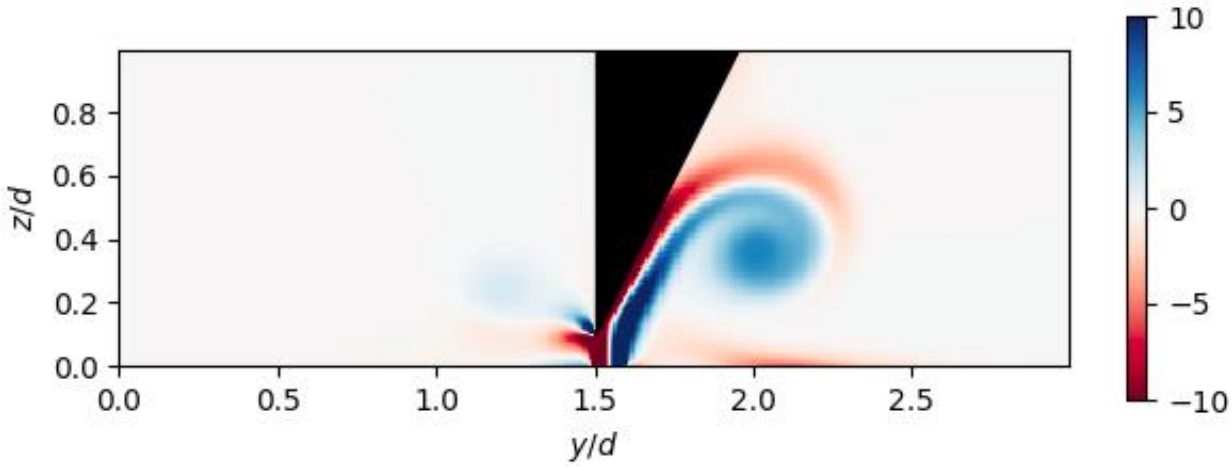

FIG 2. 1: SNAPSHOT OF VORTICITY FOR RE 1000

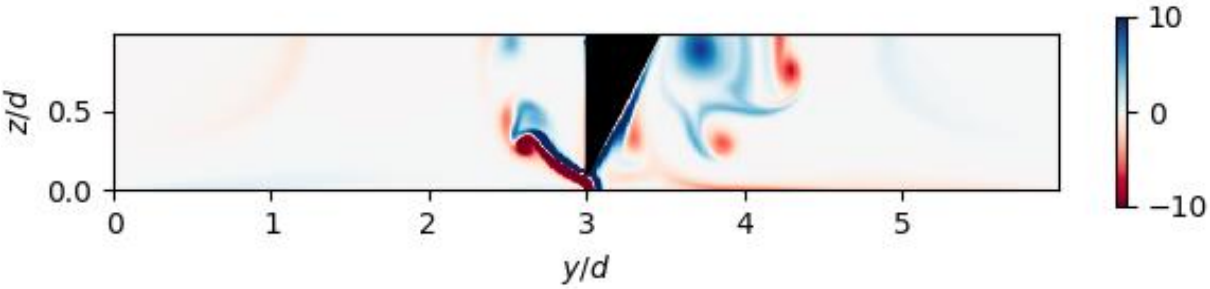

FIG 2. 2: SNAPSHOT OF VORTICITY FOR RE 4000

2.2.1 Boundary Conditions

Our computational domain is a rectangular area with four edges and has another boundary of a flute labium inside, around which the fluid flutters as shown in figures 2.2-3. The bottom of the domain is where the fluid (air) enters in form of a jet, approximately at the center of the domain. The jet is inflow of a certain velocity profile whereas, all the other region in the bottom apart from the jet is fixed at zero velocity. It is implemented using Dirichlet boundary condition. The exit boundary condition is an outflow wave propagation equation, with a prescribed Courant number. The Courant number expression is given by $du/dt + C\, du/dz = 0$ at the boundaries for every u component. C is the Courant number that governs how fast

flow traverses through the outflow boundary. The independence of the results to the Courant number are checked in a later section.

We know from intuition that the vortex grows and could hit one or both the sidewalls if they are not far enough. So, we do not want the effects of the shear layer to further interfere with our results in the simulation. Therefore, the two vertical sidewalls have a free-slip condition imposed on them. At the interface between the fluid and the wall, the tangential component of the fluid velocity is unrestricted, but the normal component is zero inhibiting penetration through the wall but allowing the fluid to 'slip' at the boundary.

As proposed by Fadlun *et al.* [21], a combined Immersed-Boundary Finite-Difference method is used to simulate the flow in the given geometry keeping the geometric integrity in mind. The labium surface is the immersed boundary in our domain of simulation. This method is second order accurate and highly efficient as it very cleverly uses forcing function on the 'immersed boundary' to describe the geometry of the flute labium without compromising the rectangular shape of the mesh or having the mesh go around the boundary of the labium.

2.3 Control parameters

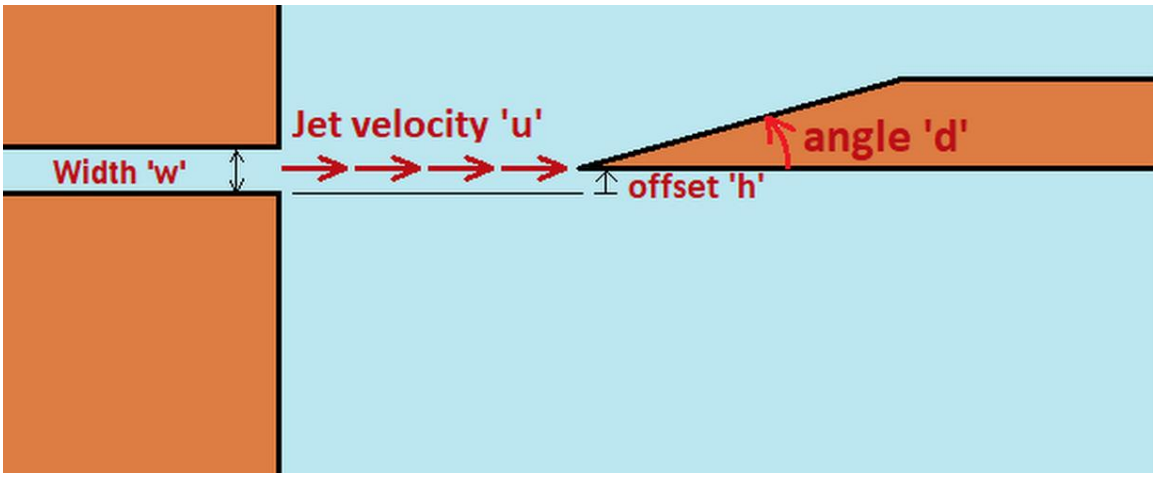

FIG 2. 3: CONTROL PARAMETERS OF THE SIMULATION

The parameters we will be varying for our simulations are jet thickness or jet width. Since the source and the labium are kept at a constant distance away for all the simulations, varying this parameter will primarily determine the ratio of the jet width to the distance between the source and the labium.

A single parameter, the Reynolds number (Re_w) is sufficient to describe the jet. This is given by uw/v. We note that this Reynolds number is different to the one obtained from non-dimensionalizing the domain using the vertical length. The values of Re_w observed in instruments like recorder flutes can be generally in the range of a few hundreds. For a given jet width, the distance between the slit, and the labium, the frequency of oscillations varies with the jet velocity which directly affects the Re_w of the jet as well.

The offset of the labium from the slit that produces the jet of air is varied and its optimal position is investigated that may produce and maintain a stable tone by providing steady oscillations of the jet around the labium.

The simulations are repeated with different sharpnesses of the flute labium. The angle of the labium is varied so as to reproduce oscillations for sharp and blunt edges. Flutes may have a variety of labium edge sharpness ranging from a large 60^{o} angle in transverse flutes to a very sharp 15^{o} angle in recorder flutes [16].

2.4 Jet Velocity Profile

Air jets are inherently unstable. Any perturbation present at the origin of the jet is convected as well as amplified downstream [7]. The jet starting as laminar at the channel exit can excite to an extent that its cohesiveness fails to keep its structure intact and the jet breaks into vortices eventually entering into turbulence. According to the approach used by Rayleigh [7], the instability of the jet that leaves the flue exit depends on its velocity profile. This velocity profile most significantly depends on the history of the flow in the channel before separation occurs as the jet exits the channel.

Thus, the jet velocity profile is very significant to understand a jet's intrinsic instability, and it becomes an important factor when we are investigating the response of the jet as it hits the flute labium. For our test cases, we have used two different kinds of velocity profiles for the incoming jet of air that grazes the labium.

2.4.1 Parabolic Velocity Profile

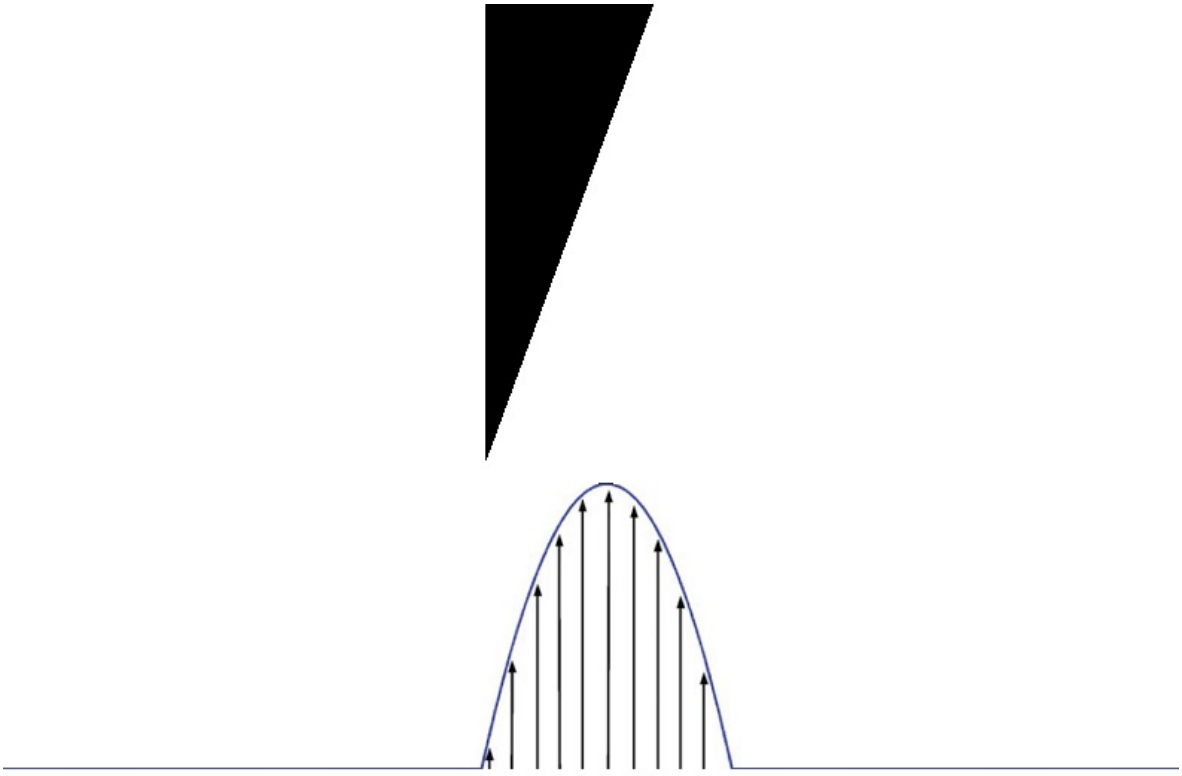

FIG 2. 4: PARABOLIC VELOCITY PROFILE OF THE JET INCIDENT ON THE LABIUM

First, we use the incoming velocity profile which would occur naturally when a fluid passes through a thin channel. While traveling inside the confined channel with constant cross-section, due to fluid's viscosity, elements closer to the wall tend to slow down creating a velocity gradient with the fluid stationary at the wall surface and the fastest in the middle of the channel. This makes the boundary layer thicker, and consequently, the velocity profile of the flow is smooth exhibiting some vorticity inside the jet. However, the channel must be long enough to give time for the complete smoothing to take place and flow to fully develop. Therefore, in this case when flow is fully developed into a parabolic profile, for non-

dimensionalization purposes we choose the characteristic velocity to be equal to the maximum velocity of the profile.

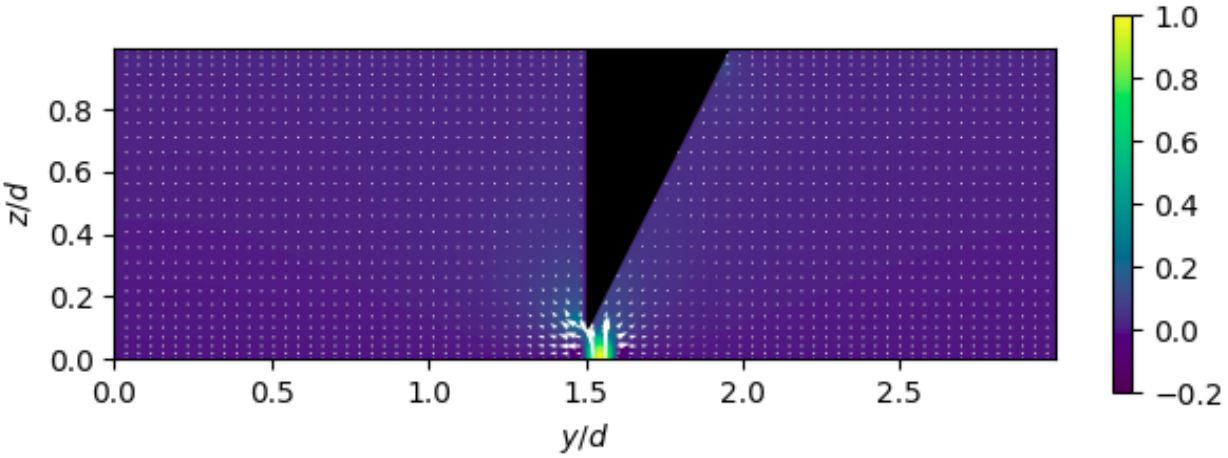

FIG 2. 5: VELOCITY PLOT FOR PARABOLIC PROFILE AT RE = 1000, JET WIDTH 0.1L, AT 26.5° LABIUM

Figures 2.5-6 are a single snapshot from the numerical simulation carried out for our investigation. It shows a parabolic velocity profile of slit width 0.1 characteristic lengths, incident on the flute labium of angle 26.5° just at 0.1 time-units of the simulation. There is smoothing of the jet visible and the jet is interacting with the fluid molecules outside of the jet as well which causes instability.

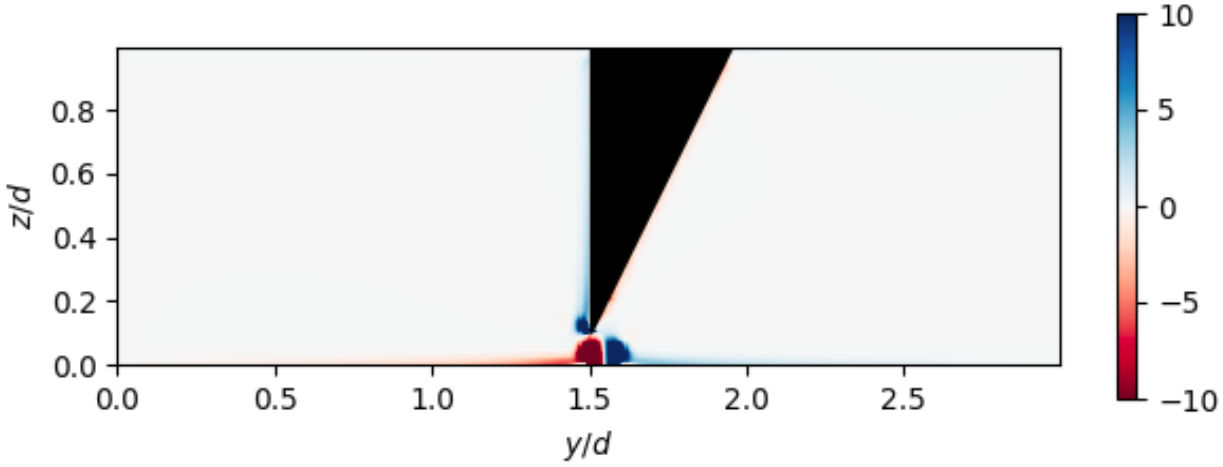

FIG 2. 6: VORTICITY FOR PARABOLIC PROFILE AT RE = 1000, JET WIDTH 0.1L, AT 26.5° LABIUM

Figure 2.6 is the corresponding vorticity plot for the velocity plot shown in figure 2.5. Looking at the vorticity of the fluid in the domain, we can see that there are no sharp discontinuities. The vorticity is in the counter phase about the middle of the jet. That is, it is clockwise on one half and counterclockwise on the other. Any perturbation will grow as it travels away up to the point where it breaks into vortices. This means that the jet is convectively unstable.

2.4.2 Uniform Velocity Profile

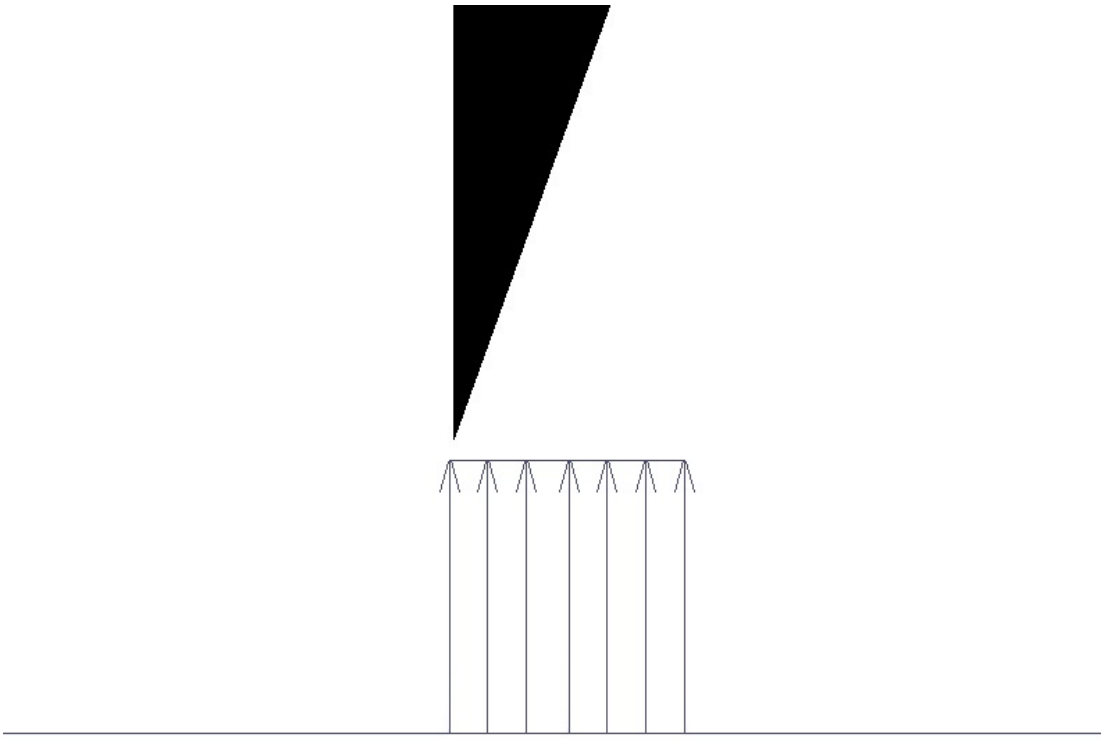

FIG 2. 7: UNIFORM VELOCITY PROFILE OF THE JET INCIDENT ON THE LABIUM

When the channel fluid passes through a channel which is not long enough, the boundary layer does not develop fully, and the velocity profile does not smooth out completely. The shorter the channel length, the less it smooths out and comes

out of the channel exit as having a top hat velocity profile. There is still however some smoothing present in the case of a short formation channel.

A uniform jet could also be thought of as the complementary inviscid limit to the parabolic profile. As all the momentum passed on to the flow is perfectly transmitted in all shear layers until the exit of the channel. Since the flow is inviscid, the jet does not tend to stick to the wall surface and the layers closer to the pipe do not slow down. In other words, the fluid does not experience any change of velocity in its transverse direction. In this case, it becomes natural to take the characteristic velocity equal to the uniform jet velocity.

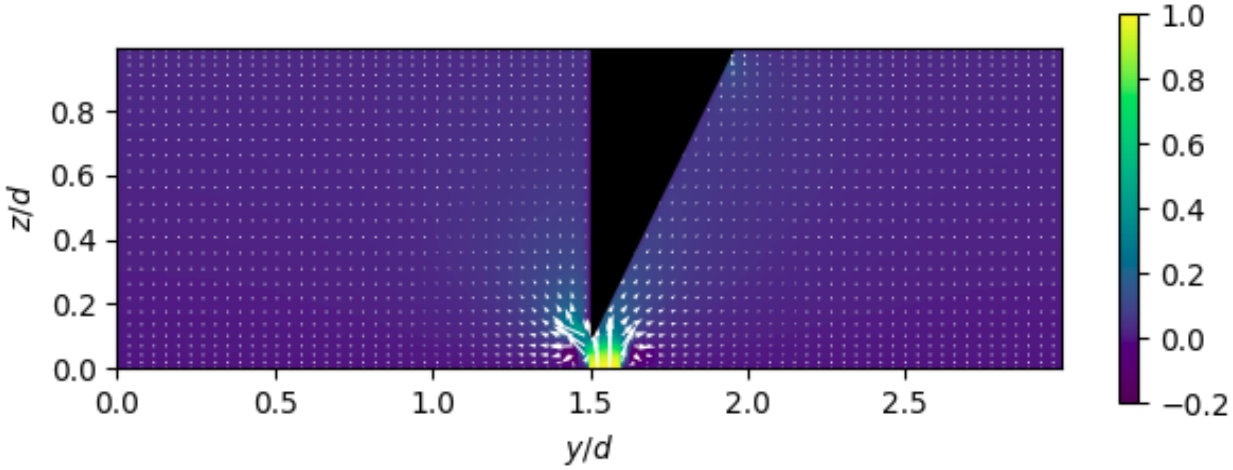

FIG 2. 8: VELOCITY PLOT FOR UNIFORM PROFILE AT RE = 1000, JET WIDTH 0.1L, AT 26.5° LABIUM

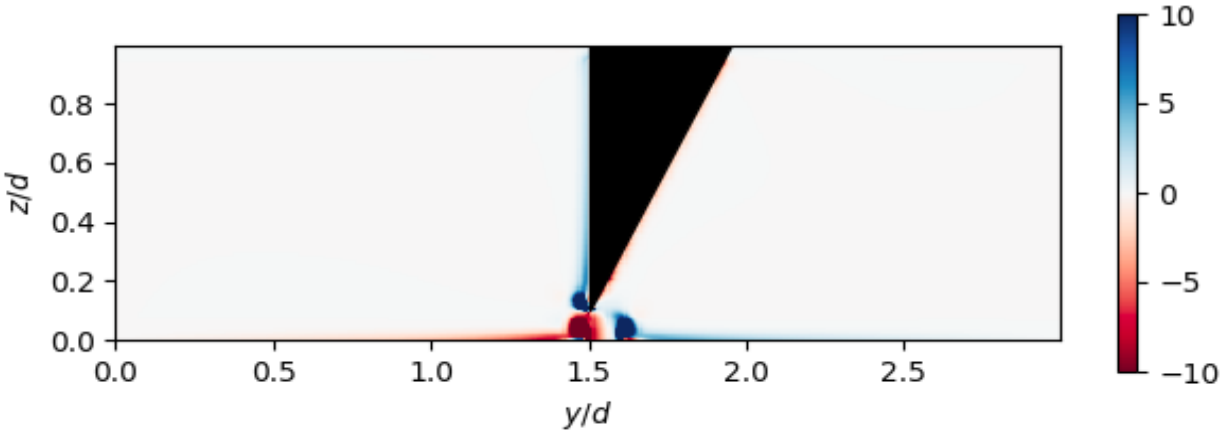

FIG 2. 9: VORTICITY FOR UNIFORM PROFILE AT RE = 1000, JET WIDTH 0.1L, AT 26.5^{o} LABIUM

Figures 2.8-9 here show uniform velocity profile of width 0.1 incident on the flute labium of angle 26.5^{o} at 0.05s of the simulation. The velocity discontinuity at the jet's edge will have smoothing going on as it leaves the flue exit. The molecules outside of the jet are also beginning to interact with the jet resisting its flow and peeling it back. This causes perturbations and makes the jet more likely to roll up into a vortex. The vorticity of the domain confirms that the velocity profile is constant as there is no vorticity inside the jet. However, the presence of a strong vorticity just outside of the jet predicts the likelihood of instability and vortex formation.

3. Results

Several test case simulations are run for different parameters. First, the effects of Reynolds number on the oscillations of the jet will be detailed. For this case the angle is set at arctan(1/2), the width of the jet is 0.1, the position of the jet is such that the left hand side of the jet is aligned with the left hand side of the flute labium. For all the cases, the Courant number is fixed at 0.4.

3.1 Effect of Reynolds Number

3.1.1 Reynolds Number 500

At this Reynolds number, the jet of air fails to produce oscillations around the flute labium. There is however a transient, faint momentary flutter around the edge, but the Reynolds number is too low to sustain an oscillation. The flow just grazes against the labium surface and a growing boundary layer is witnessed. Flow instability is not enough to cause perturbations sufficient to reverse the flow hence there is no oscillation. This case is similar to fluid flowing over a flat plate with boundary layer developing as the fluid travels downstream.

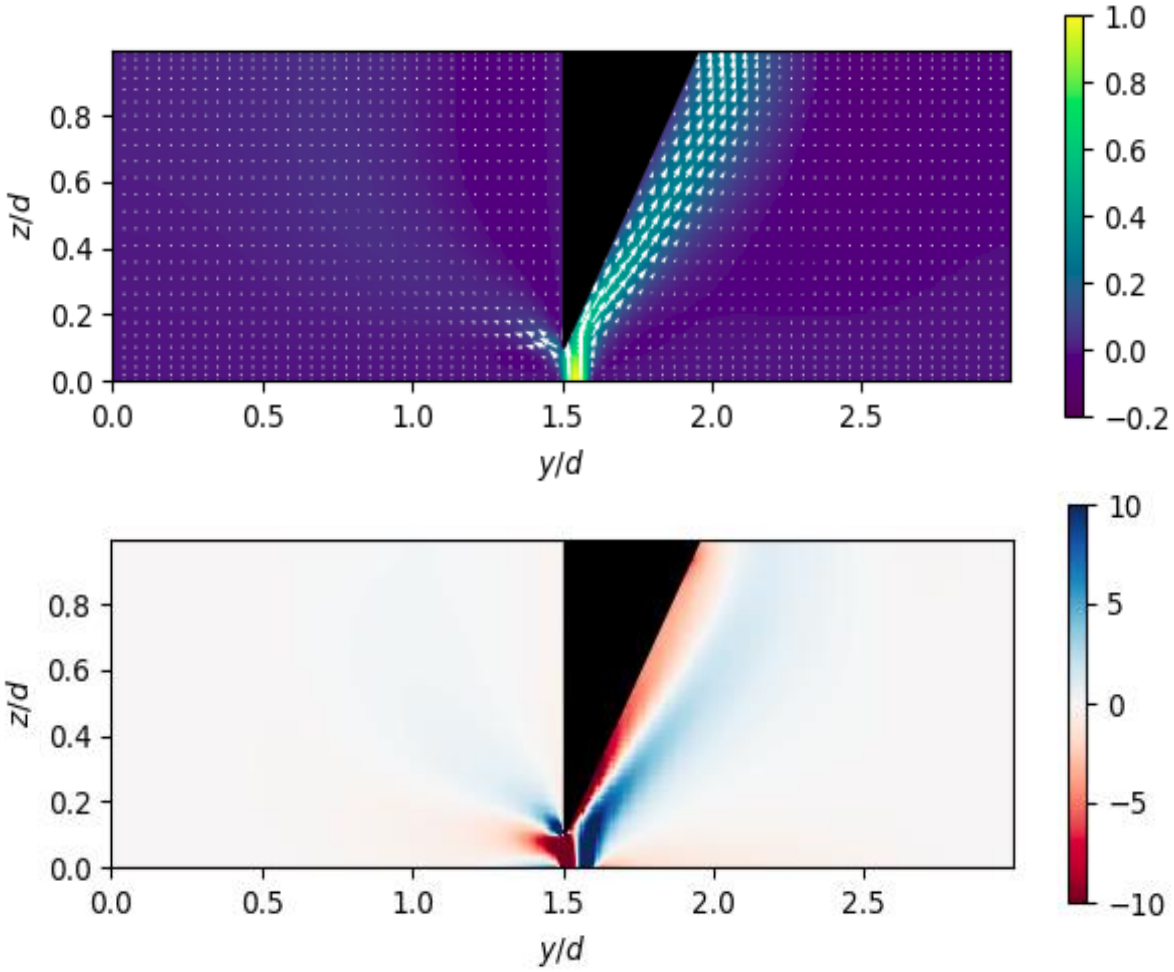

FIG 3. 1: VELOCITY(TOP) AND VORTICITY(BOTTOM) OF THE FLUID AT STEADY STATE FOR RE=500, AND JET WIDTH 0.1L

3.1.2 Reynolds Number 1000

An increase in Reynolds number to 1000 produces very consistent oscillations. These oscillations have a period of 0.86 time-units. Figures 3.2-3 show the time sequence of how the jet evolves and sheds vortex as it hits the labium and starts to alternate its direction from one side of the labium to the other.

t=1.8

t=0.4

t=1.0

t=1.3

t=1.8

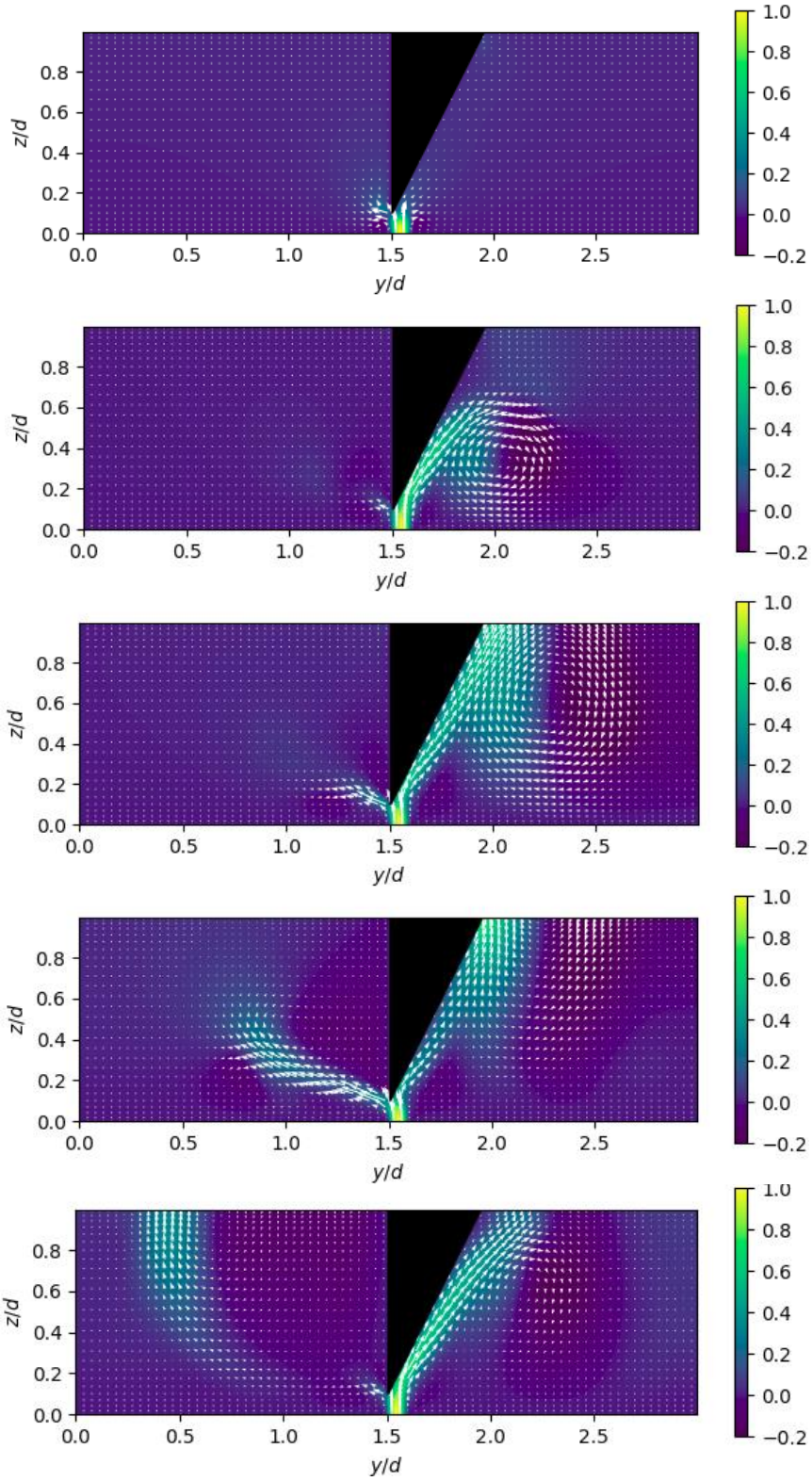

FIG 3. 2: TIME SEQUENCE OF THE VELOCITY PROFILE, AS THE JET OF AIR FLUTTERS AROUND THE LABIUM. RE=1000, JET WIDTH=0.1L

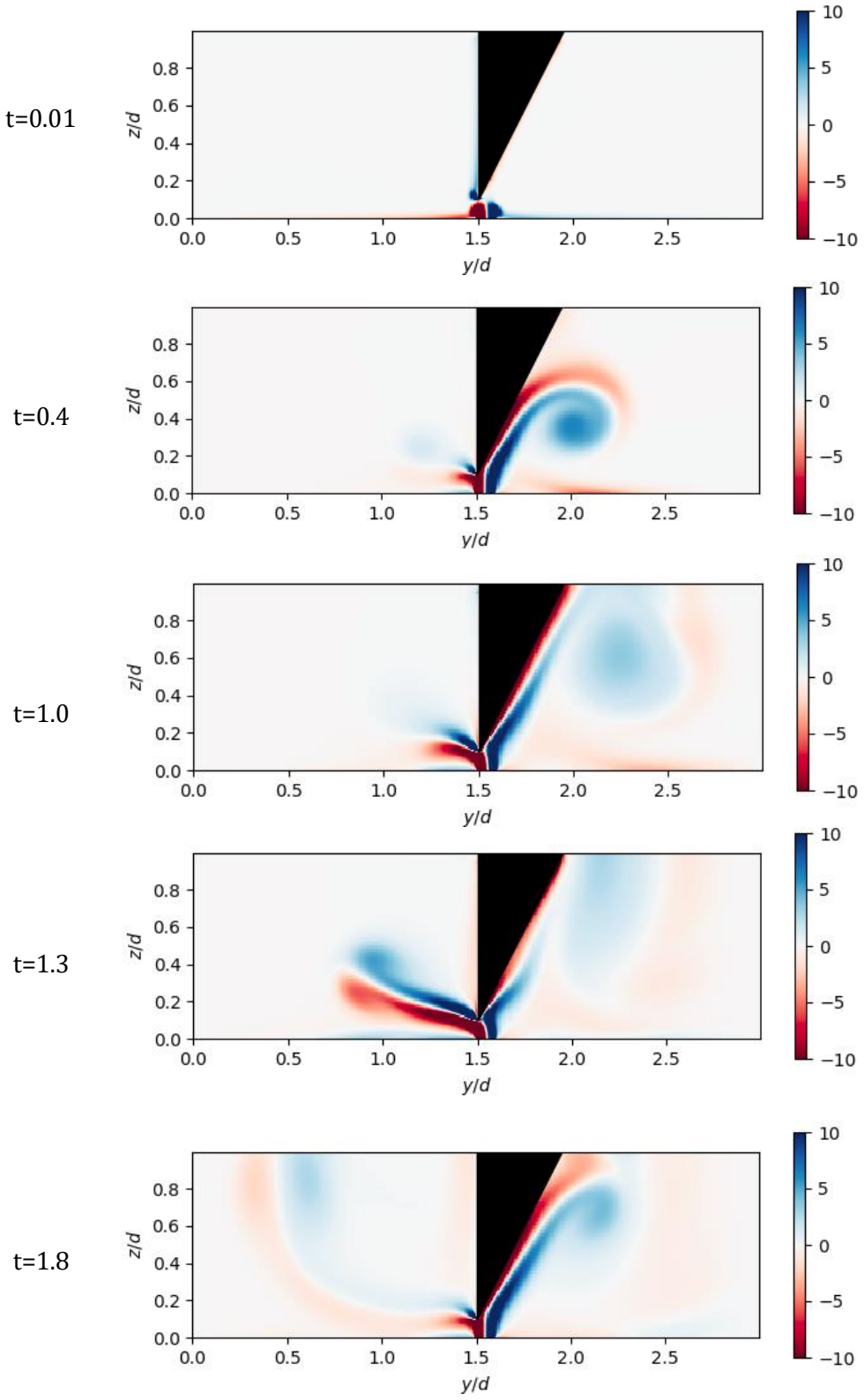

FIG 3. 3: TIME SEQUENCE OF THE VORTICITY, AS THE JET OF AIR FLUTTERS AROUND THE LABIUM. RE=1000, JET WIDTH=0.1L

As the fluid travels across the surface of the labium, because of the inclination of the labium, the fluid experiences a shortening of passage it is traveling through and thus a positive pressure gradient is present which increases the fluid velocity. At the tip of the labium, a fraction of the fluid keeps flowing to the other side of the labium as it attaches to the surface. At the same time a vortex is formed on the inclined side which continues to grow. The vortex is formed because the moving fluid creates a low-pressure zone and the adjacent stationary fluid starts to travel to the low-pressure area creating an angular momentum This vortex continues to grow until it finally dissipates, and the jet of air reattaches to the surface of the labium causing a sudden drop in the velocity. This results in the back flow of the jet and the flow changes its direction. When the flow on the inclined side normalizes, the jet then continues on this side and forms a vortex again. This results in a sustained oscillatory motion.

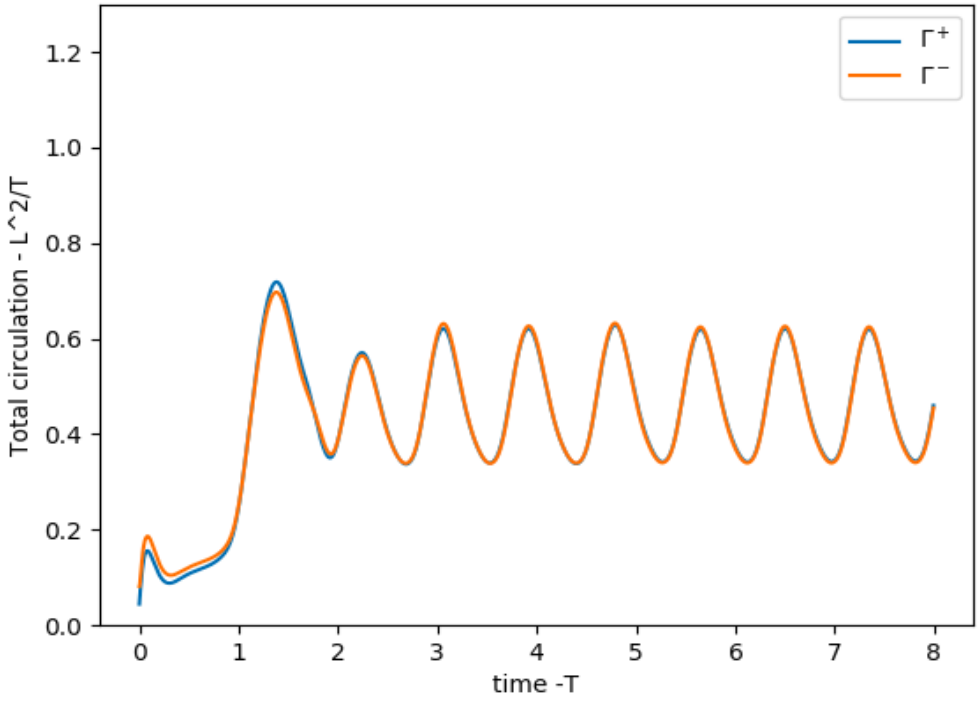

FIG 3. 4: CIRCULATION (CLOCKWISE '+' AND ANTICLOCKWISE '-') OF FLUID AT LEFT SIDE OF THE LABIUM, RE=1000, JET WIDTH=0.1L

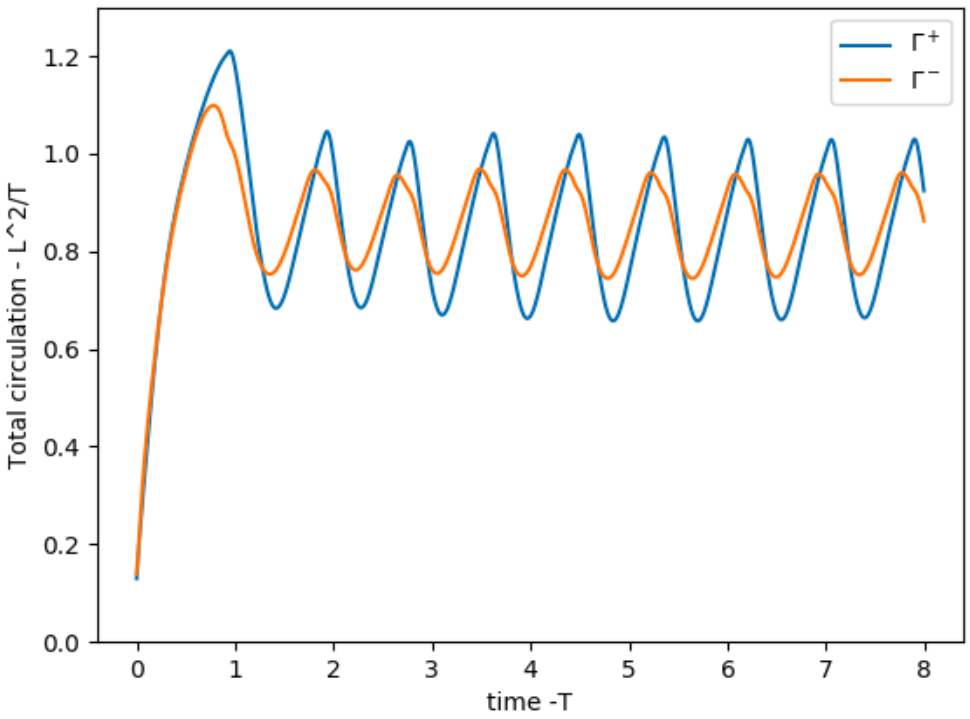

FIG 3. 5: CIRCULATION (CLOCKWISE '+' AND ANTICLOCKWISE '- ') OF FLUID AT RIGHT SIDE OF THE LABIUM, RE=1000, JET WIDTH=0.1L

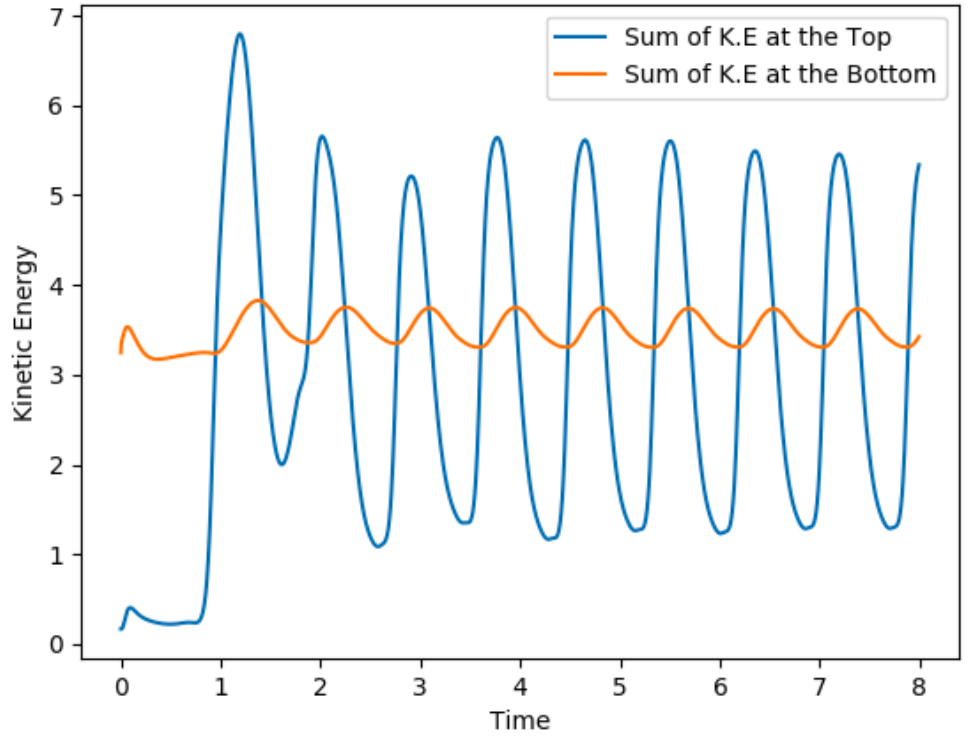

FIG 3. 6: SUM OF KINETIC ENERGIES IN Y AND Z-DIRECTIONS AT THE TOP (EXIT) AND BOTTOM (INFLOW), RE=1000, JET WIDTH=0.1L

The total circulation of the fluid at each side and the sum of the kinetic energies of the fluid elements at top and bottom of the labium oscillate as the jet changes direction from one side of the labium to the other. When the circulation at right side is maximum, it is minimum on the left side of the labium and vice versa. The time period between these peaks is measured and averaged to find a mean period of oscillations. For this case, the period of oscillation is 0.86 time-units.

3.1.3 Reynolds Number 2000

Similar to the case of Reynolds number 1000, some flow is bled to the straight side of the labium edge. The fluid initially continues to travel over the inclined surface of the labium simultaneously forming a vortex. The vortex grows and dissipates just as it does at the lower Reynolds number of 1000. The dissipation of the vortex results in back flow and thus reverses the flow to the straight side of the labium, followed by a sustained oscillation of the jet. In this case however, due to higher Reynolds number, the momentum of the flow is higher and thus the fluid continues in the direction of the inclined side for a slightly longer period than for the lower Reynolds number case until it changes its direction. This also results in a longer period of oscillation for this case.

A closer inspection of the vorticity of the fluid shows subsequent generation of mini vortices similar to Figure 3.9 with the main vortex body. This implies a higher instability of the jet. The increasing total circulation at each side of the labium as shown in Figures 3.7-8 confirms this increasing instability and production of more vortices.

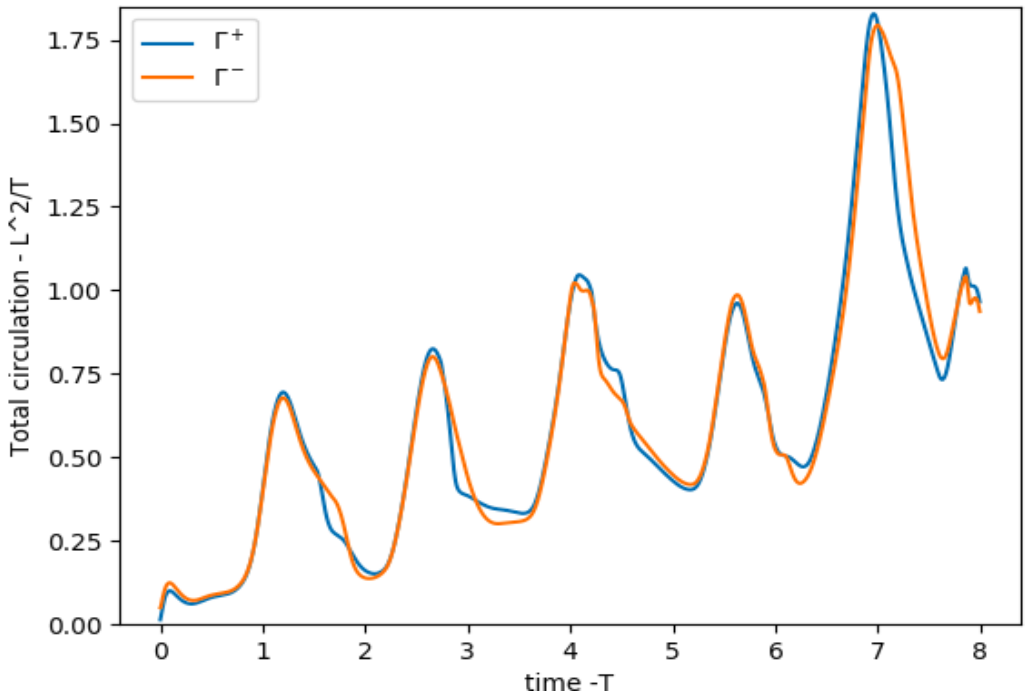

FIG 3. 7: CIRCULATION (CLOCKWISE '+' AND ANTICLOCKWISE '-') OF FLUID AT LEFT SIDE OF THE LABIUM, RE=2000, JET WIDTH=0.1L

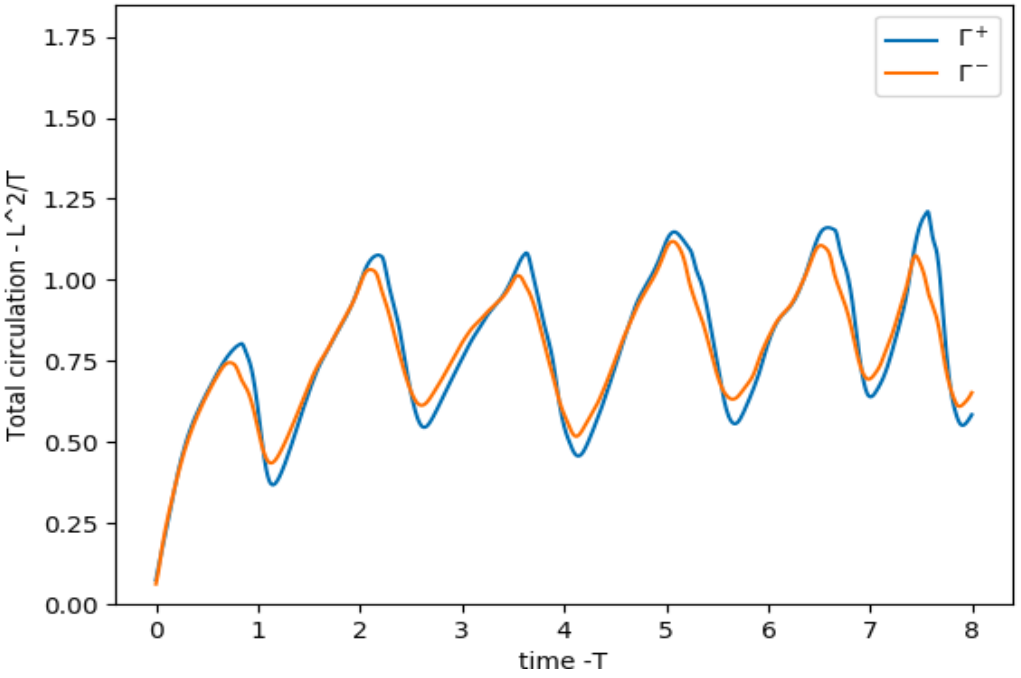

FIG 3. 8: CIRCULATION (CLOCKWISE '+' AND ANTICLOCKWISE '-') OF FLUID AT RIGHT SIDE OF THE LABIUM, RE=2000, JET WIDTH=0.1L

The oscillations in this case are still fairly consistent with a repeatable period. The period of oscillations observed for this Reynolds number is about 1.46T.

3.1.4 Reynolds Number 4000

Further increasing the Reynolds number introduces instabilities and the flow regime moves towards turbulence. The flow no longer maintains its laminar integrity. Even though the flow changes direction when the main vortex dissipates, the behavior of the fluid is very erratic producing much stronger vortices and it is difficult to predict the change of direction of fluid from one side of the labium to the other as there are further small vortices formed in the domain as well. These smaller vortices interact with the main incoming flow as well and affect the period of oscillation.

The flow tends to return back to the original side of attack i.e. the inclined side on the right. The flow still keeps oscillating at roughly the period of around 1.38T. Figure 3.8 shows flow vorticity plot at 0.8T. The flow is about to reverse and be directed to the left side of the labium. It also shows the formation of smaller vortices and shows that they interact with the main flow. The labium induces an excitation with an increasingly broad frequency range as the Reynolds number increases.

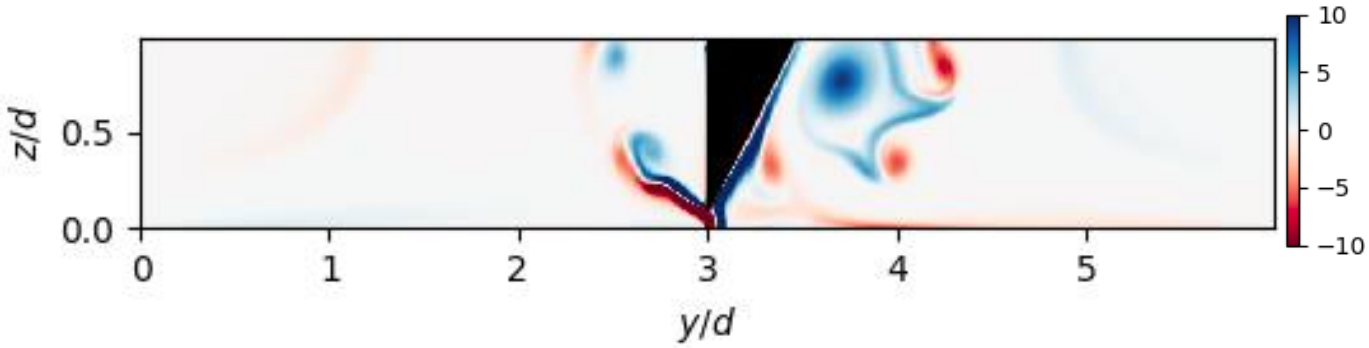

FIG 3. 9: VORTICITY OF FLUID IN THE DOMAIN AT 0.8T SHOWING THE SUBSEQUENT PRODUCTION OF SMALLER VORTICES WHICH ARE INTERACTING WITH THE MAIN FLOW

3.2 Effect of Jet Width

The oscillations produced for the jet width of 0.1L were fairly stable at Reynolds number around 1000 and the jet produced no oscillations at all at a low Reynolds number of 500. To investigate the effect of the width of the jet on the oscillations, we decreased the jet width to half its size in the previous cases i.e. 0.05L, and in one case increased it to 0.2L. For the bigger jet width of 0.2 L we only simulated for one case of Re 500 which did not produce any oscillations. Our main focus is however on the smaller jet width for this section. For the jet width of 0.05L, we observe that reducing the jet width generally reduces the period of oscillations around the labium as well.

We kept the distance between the labium and flue exit the same in all the simulations, so changing the jet width changes the ratio of the jet width to this distance. This distance itself also has an effect on the stability of the flute with respect to the labium but observing the response for changing the length of the jet, we do not expect this effect to be too great.

3.2.1 Re 500, Width = 0.05

At a low Reynolds number of 500, we still do not observe any oscillation. There is no transient change of direction from one side of the labium to the other like in the case of jet width of 0.1. The flow maintains a steady state profile over the labium which does not change with time. Like in the case of 0.1L jet width, the Reynolds number is not big enough for the inherent instabilities in the jet to incite oscillations at the labium.

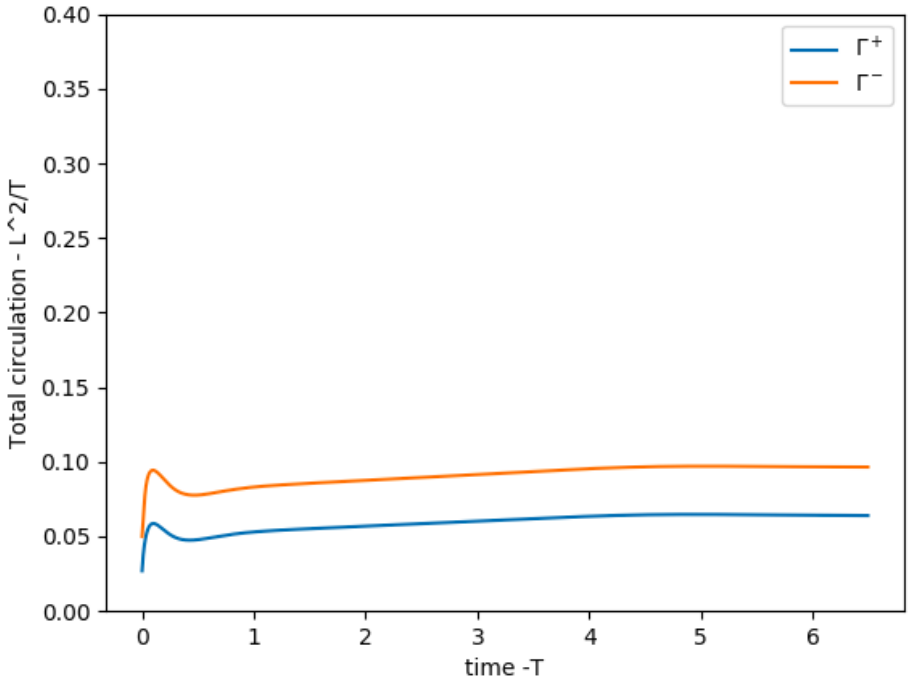

FIG 3. 10: CIRCULATION (CLOCKWISE '+' AND ANTICLOCKWISE '-') OF FLUID AT RIGHT SIDE OF THE LABIUM, RE=500, JET WIDTH=0.05L

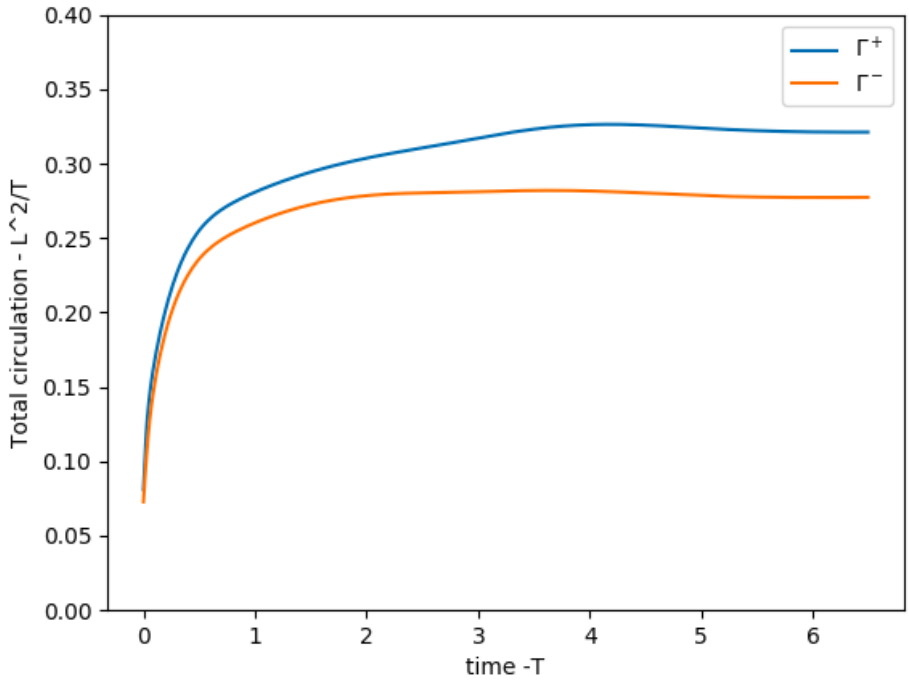

FIG 3. 11: CIRCULATION (CLOCKWISE '+' AND ANTICLOCKWISE '-') OF FLUID AT LEFT SIDE OF THE LABIUM, RE=500, JET WIDTH=0.05L

3.2.2 Re 1000, Width=0.05

Increasing the Reynolds number to 1000 makes the flow exhibit oscillations. The oscillations are more subtle as compared to the same Reynolds number at higher jet width. The vorticity as well as the difference in maximum and minimum vorticities is not as high as in the case of thicker jets, indicating that the vortex is not as strong, and it does not dissipate as quickly either. The oscillations are such that a fraction of the bulk of the flow maintains the flow profile attached to the labium surface while the other part of the flow swings around the labium. The period of oscillation for the case is quantified to be 0.62T. Since the jet width is smaller, the resistance to any perturbation to the flow is smaller too. This results in the perturbations getting amplified to a higher degree for the same length scale. Thus, at the labium the flow oscillates more frequently.

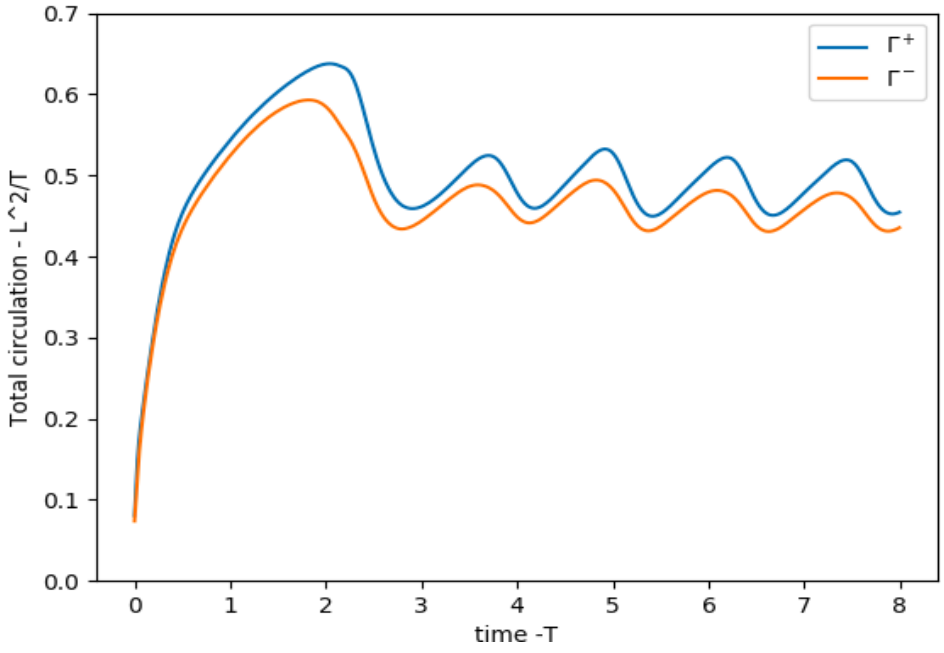

FIG 3. 12: CIRCULATION (CLOCKWISE '+' AND ANTICLOCKWISE '-') OF FLUID AT RIGHT SIDE OF THE LABIUM, RE=1000, JET WIDTH=0.05L

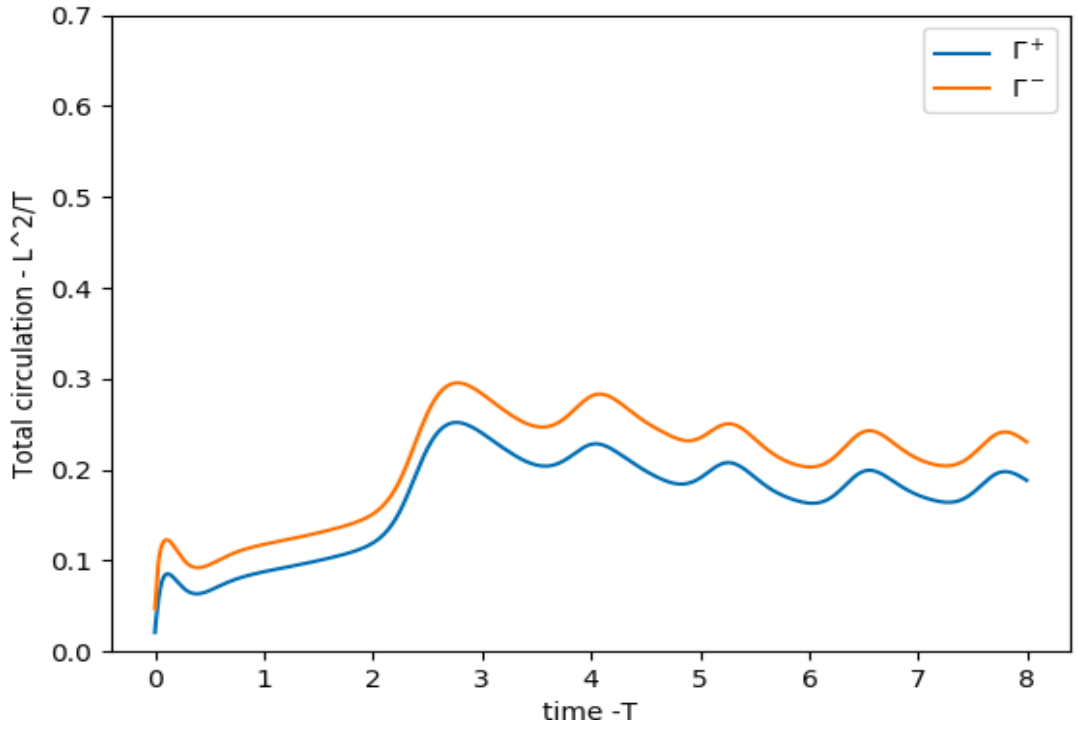

FIG 3. 13: CIRCULATION (CLOCKWISE '+' AND ANTICLOCKWISE '-') OF FLUID AT LEFT SIDE OF THE LABIUM, RE=1000, JET WIDTH=0.05L

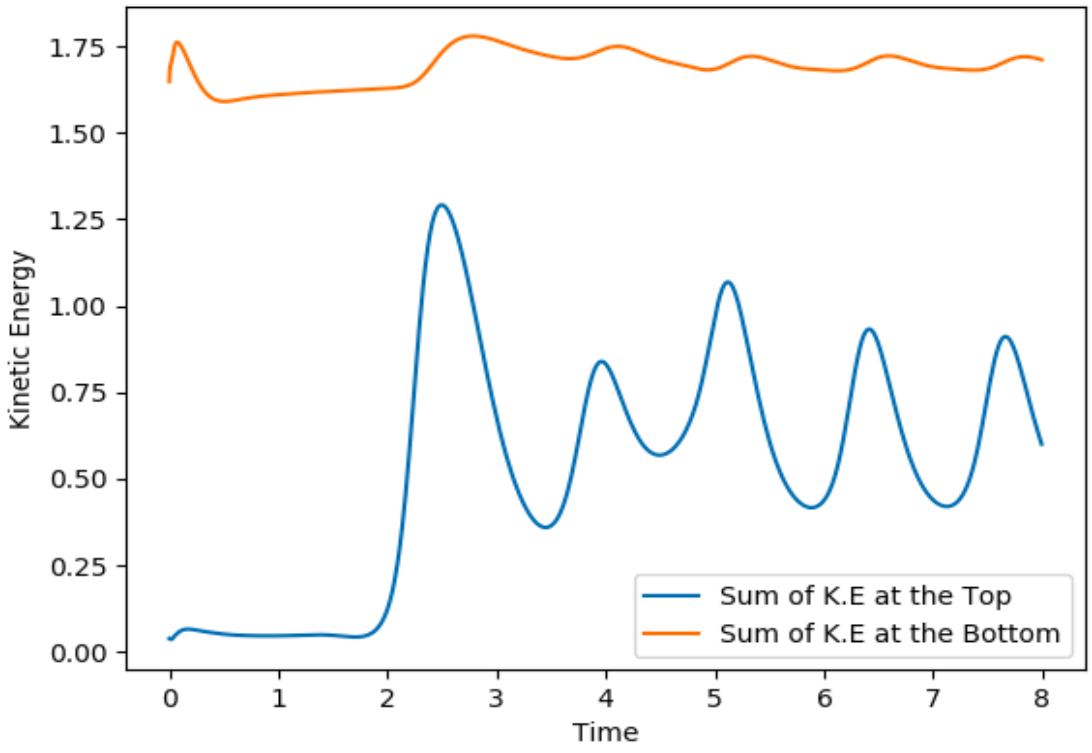

FIG 3. 14: SUM OF KINETIC ENERGIES IN Y AND Z-DIRECTIONS AT THE TOP (EXIT) AND BOTTOM (INFLOW), RE=1000, JET WIDTH=0.05L

3.2.3 Re 2000, Width=0.05

Increasing Reynolds number further makes the oscillations more pronounced and visible from the lower Re numbers. More bulk of the jet oscillated around the labium. As compared to the jet width of 0.1, the period of oscillation is lowered as well from 1.46T to about 1.1T in this case.

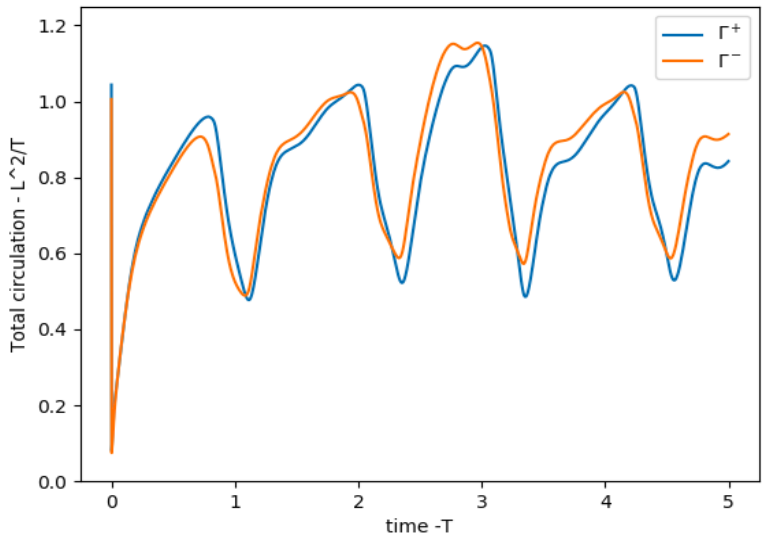

FIG 3. 15: CIRCULATION (CLOCKWISE '+' AND ANTICLOCKWISE '-') OF FLUID AT RIGHT SIDE OF THE LABIUM, RE=2000, JET WIDTH=0.05L

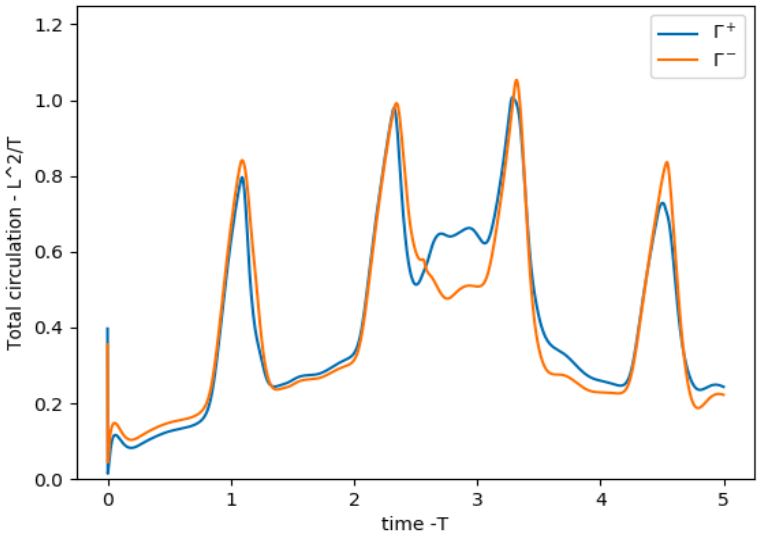

FIG 3. 16: CIRCULATION (CLOCKWISE '+' AND ANTICLOCKWISE '-') OF FLUID AT LEFT SIDE OF THE LABIUM, RE=2000, JET WIDTH=0.05L

We note that the effect of making the channel smaller is counterintuitive. While one could expect at first that the timescale becomes faster because the length-scale is smaller, what happens is that the oscillation timescales become longer.

3.3 Effect of slope of labium

The effects of changing the sharpness of the labium are studied. The simulations performed in previous sections were done on a flute labium of an angle of about 26.5 degrees. We have repeated the simulations for two more angles of labium cases: 14 degrees and 45 degrees. A comparison of the oscillation period of these different slopes of labium will give us an idea of the behaviour of the flow more clearly.

3.3.1 14-degree labium angle

Most recorder flutes have a labium angle of about 15 degrees which is very close to the angle in this case of our simulation. Sharpening the angle of the labium reduces the distance between the vortices are formed at each side of the labium. Thus, it is expected to give rise to more impulsive vortex shedding. The simulations are carried out at different Reynolds numbers and jet widths for this angle. Figure 3.13 (on next page) shows the evolution with time of jet of 0.1L width and 1000 Reynolds number incident on the 14-degree labium.

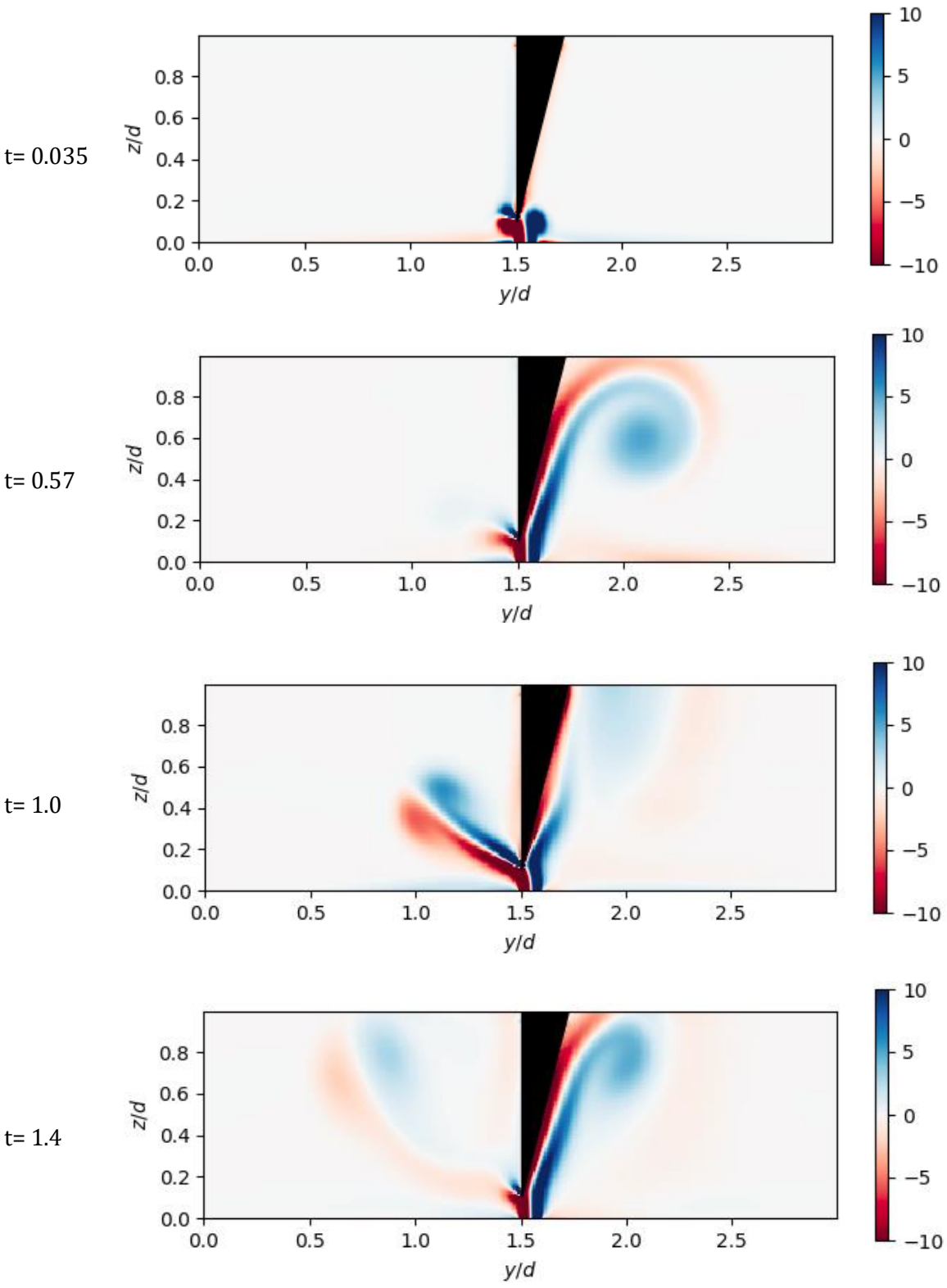

FIG 3. 17: TIME SEQUENCE OF VORTICITY OF FLOW OVER THE 14⁰ LABIUM, RE=1000, JET WIDTH=0.1L

Figure 3.17 shows the formation of vortex, its dissipation, and the reversal of flow to the left side of the labium for a jet width of 0.1L and Reynolds number 1000. The jet then regains its momentum in the right side of the labium, and the process repeats itself continuously. For this particular case, the period of oscillations is 0.77T which is lower than the period in our previous simulations with a less sharp labium of angle 26.5^{o} and same jet width and Reynolds number.

As expected for sharpening the labium angle, this trend of lower period of oscillation is also observed for the jet width of 0.05L at Re 2000 due to impulsive vortex shedding. At a low Reynolds number of 500, we do not observe any oscillations for this sharp angle of labium as well. A comparison of the periods of oscillation for different jet widths and Reynolds numbers is given in figures 3.14 -15.

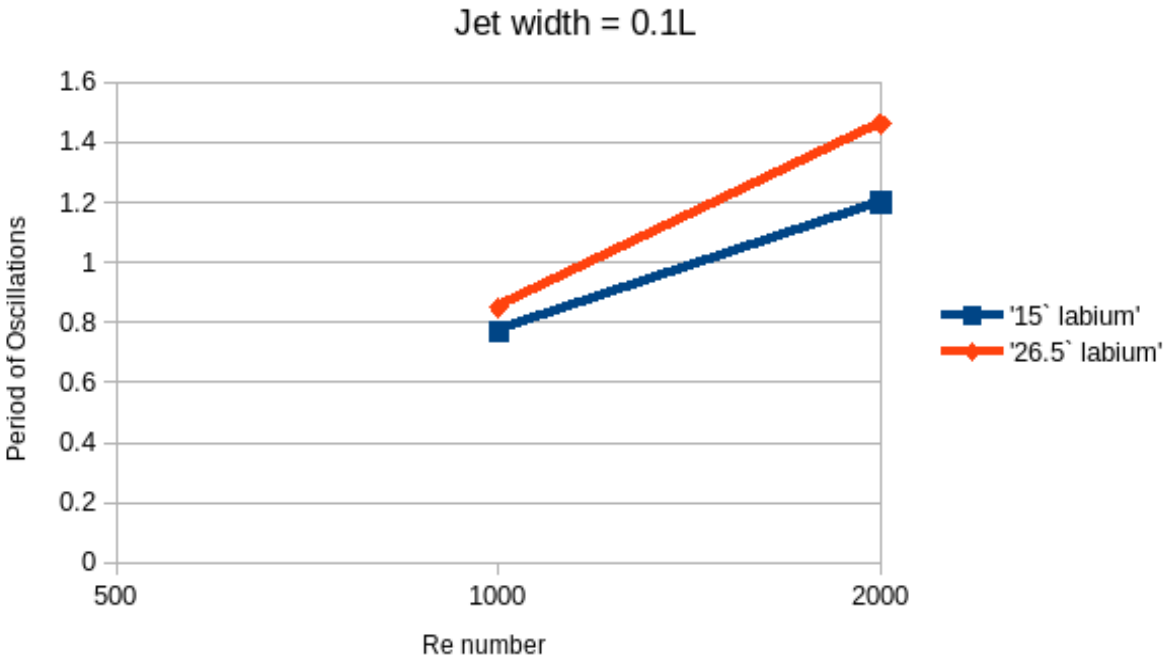

FIG 3. 18: COMPARISON OF PERIOD OF OSCILLATION AT DIFFERENT RE NUMBERS FOR 15^{o} AND 26^{o} LABIA FOR 0.1L JET WIDTH

TABLE 3. 1: PERIOD OF OSCILLATION FOR 14° AND 26.5° LABIA AT DIFFERENT RE NUMBERS

Jet Width	Re number	15 deg labium	26.5 deg labium
0.1	500	no oscillation	no oscillation
	1000	0.77	0.85
	2000	1.2	1.46

FIG 3. 19: COMPARISON OF PERIOD OF OSCILLATION AT DIFFERENT RE NUMBERS FOR 15° AND 26° LABIA FOR 0.05 JET WIDTH

TABLE 3. 2: PERIOD OF OSCILLATION FOR 14^o AND 26.5^o LABIA AT DIFFERENT RE NUMBERS

Jet Width	Re number	15 deg labium	26.5 deg labium
0.05	500	no oscillation	no oscillation
	1000	0.53	0.62
	2000	0.81	1.1

3.3.2 45-degree labium angle

For the 45-degree labium angle, the jet remains relatively stable for low Reynolds numbers of 500 and 1000. There are no oscillations observed for these Reynolds numbers neither for both the jet widths we simulated for. Figure 3.16 shows the interaction of the jet, of Re 1000 and width 0.1L, with the labium of 45-degree angle. The incident jet sets in a steady state position with the flow on each side of the labium.

We note that the inflow conditions are probably playing a large role for this geometry, as we can see how the vortices attach themselves to the lower boundary condition. More investigation on this large-angle labium is needed to properly assess the impact of the sidewall.

t= 0.02

t= 1.8

t= 2.5

t= 5.0

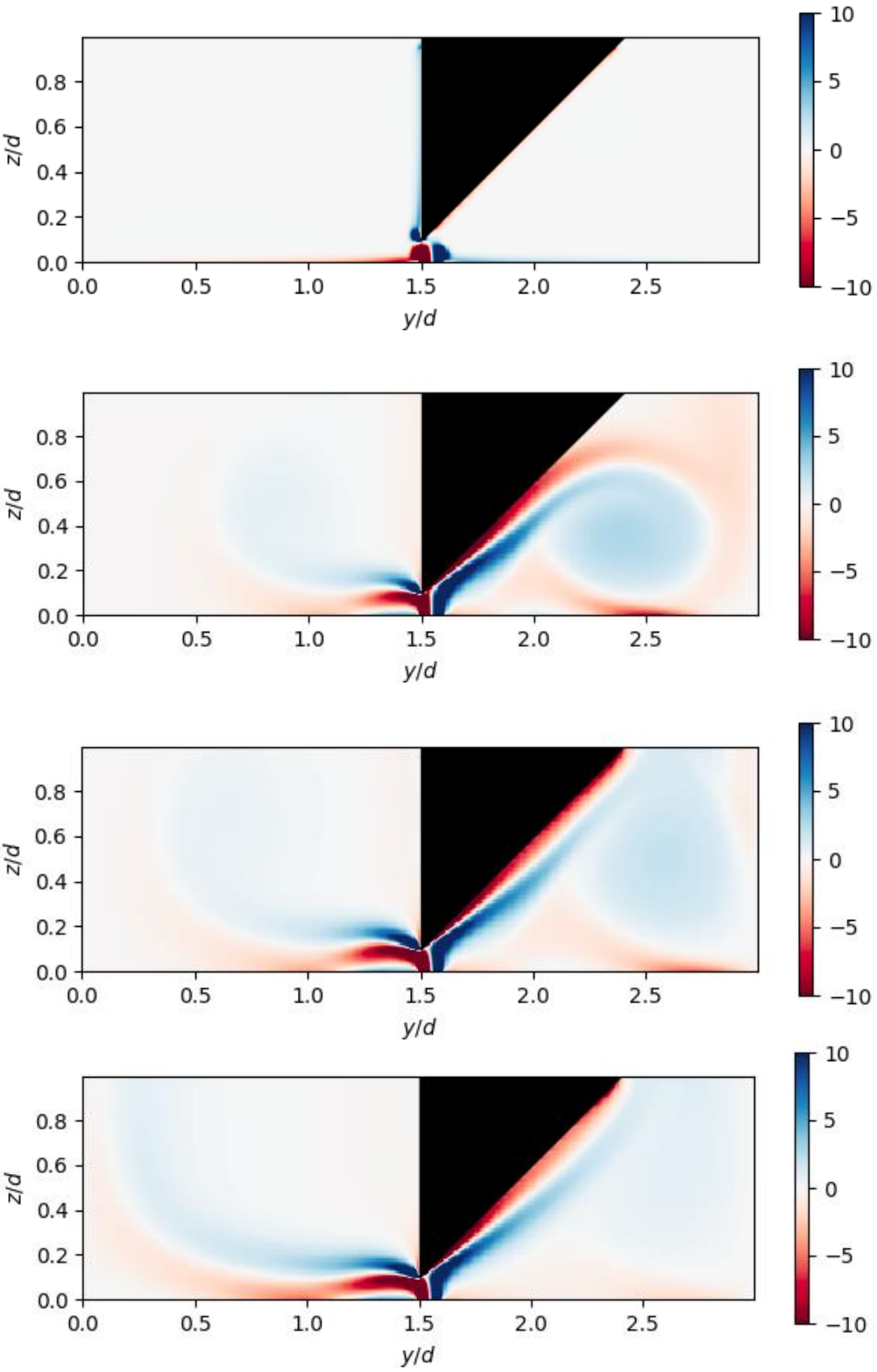

FIG 3. 20: TIME SEQUENCE OF VORTICITY OF FLOW OVER 45` LABIUM AT RE 1000 AND 0.1L JET WIDTH

3.4 Effect of velocity profile

When we change the velocity profile at the flue exit from parabolic configuration to uniform (top hat) configuration, we see a remarkable difference in the behavior of flow.

3.4.1 At Jet Width 0.1

For jet width 0.1L, starting from a low Reynolds number of 500 we see no oscillations and the jet settles in a steady state position at the labium. At Reynolds number 1000, the jet starts to oscillate but it fails to sustain any oscillations produced and the oscillations quickly die away after a few flutters. The flow reaches steady state exhibiting a simple flow of the jet of air over the inclined side of the labium with an increasing boundary layer downstream of the flow.

This is different from what we observed in the case of parabolic jet. The parabolic jet contains vorticity, and when it impacts the labium, it generates a boundary layer which has vorticity of the opposite sign. This can cause an immediate lift-off and generate a vortex dipole. The uniform jet does not contain vorticity in the jet, so it does not form a dipole with the boundary layer, just a normal boundary layer thus making impulsive vortex shedding more difficult.

The only case that does produce oscillations is when the Reynolds number is 2000 in our simulation. The instability is seen to have been increased a lot as well with multiple vortices forming alongside a main vortex. The oscillation exhibits a consistent period of an average of 1.46T. At an even higher Reynolds number i.e.

4000 in our simulation, the instability rises immensely producing chaotic turbulent flow around the labium with numerous vortices being produced and interacting with the incoming jet.

Table 3.3 below shows the period of oscillations for slit width 0.1L at different Re numbers and compares the periods for Uniform and Parabolic velocity profile configurations.

TABLE 3. 3: COMPARISON OF OSCILLATION PERIOD FOR UNIFORM AND PARABOLIC VELOCITY PROFILES

Jet width	Re number	Period/Parabolic	Period/Uniform
0.1	500	no oscillation	no oscillation
	1000	0.85	no oscillation
	2000	1.46	1.465
	4000	1.38	chaotic instability

3.4.2 At Jet Width 0.05

When the jet width is halved i.e. 0.05L, the simulations show a very interesting and remarkable difference. At Reynolds number of 500, we still see no oscillation at all. At Reynolds number of 1000, unlike the case of 0.1L jet width, we see oscillations that are stable and that do not die away after some time. Even

though the uniform velocity profile makes immediate vortex shedding a little harder, the greater amplification of the perturbations in the jet at the tip of the labium allow consistent oscillations. The period of these oscillations is 1.19T.

Further increasing the Reynolds number in our simulation results in an increase in the instability and a slight decrease in the period of oscillations. At Reynolds number 2000, the period of oscillations observed in our simulation is 0.98T. Table 3.4 shows the period of oscillations for slit width 0.05L at different Re numbers and compares the periods for Uniform and Parabolic velocity profile configurations.

TABLE 3. 4: COMPARISON OF OSCILLATION PERIOD FOR UNIFORM AND PARABOLIC VELOCITY PROFILES

Jet width	Re number	Period/Parabolic	Period/Uniform
0.05	500	no oscillation	no oscillation
	1000	0.62	1.19
	2000	1.1	0.98

3.5 Effect of offset with respect to the jet

The position of the labium with respect to the jet plays a very important role in the oscillation. To study this effect, we have simulated for an additional 3 configurations of the jet offset to the labium than what we did in the previous

sections. The Reynolds number is kept at 1000, the jet width at 0.1L, the angle of the labium is 26.4^{o}, and the position of the labium relative to the jet is varied to study its effect.

In our previous sections, all the cases we studied had the jet incident on the labium where the straight side of the labium would be in line with the left boundary of the jet. We call the distance between the left edges of the labium and the jet 'h' and use this length as a measure of the offset. Then all the simulations in our previous cases would have an offset of 0.

The additional configurations of the labium and jet offset are:

3.5.1 Case-I:

Offset 'h' = -0.1 is shown in Figure 3.17. In this case the jet of air has its right end in line with the left side of the labium. Therefore, the jet is only incident on the straight uninclined side of the labium opposite to the cases simulated in the previous sections. For this offset value, unlike the case with zero offset, we observe no oscillations. There is no flow separation, and the jet attaches itself to the flat side of the labium. The initial vortex dissipates with time bringing the flow to a steady state.

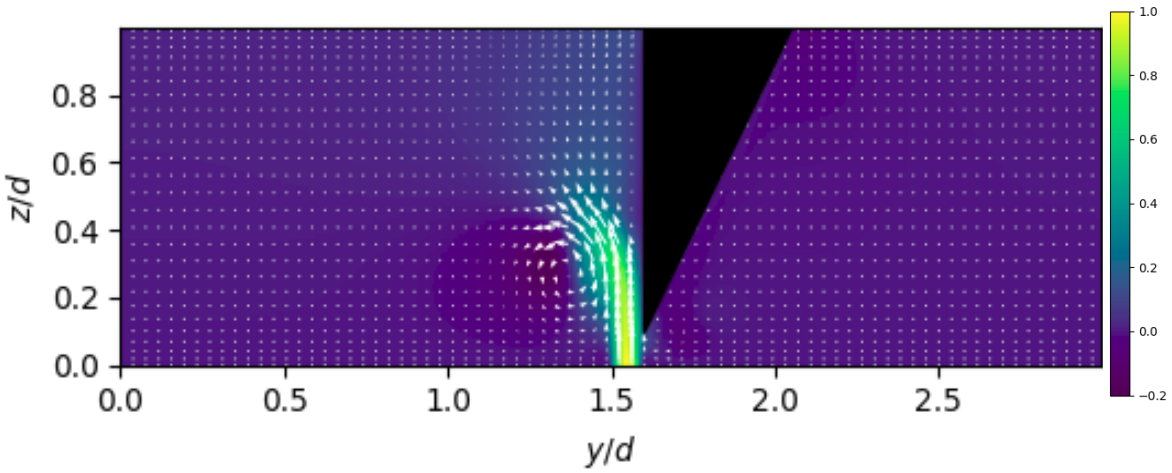

FIG 3. 21: CASE-I WITH H=-0.1

3.5.2 Case-II

Offset 'h' = -0.038. For this offset the jet is incident about halfway at the sharp corner of the labium. The sharp corner is approximately in the middle of the jet and the flow is cut through by the flute labium. The configuration is shown in Figure 3.18. The flow is separated at the tip of the labium and two simultaneous, but asymmetric vortices are shed one at each side of the labium. This asymmetry instantly induces oscillations that have a small period as tabulated in Table 3.5

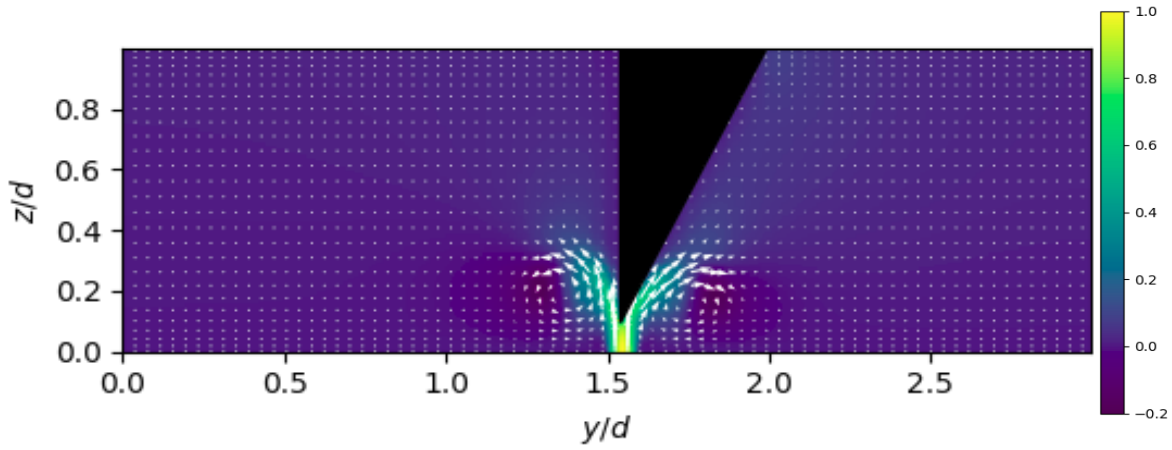

FIG 3. 22: CASE-II WITH H=-0.04

3.5.3 Case-III

For this case shown in Figure 3.19, the offset is about 0.036. The jet is incident on the inclined side of the labium with the distant h from the corner as shown in the figure below. This increases the distance from the tip of the labium to the jet. Consequently, the jet has to travel more to complete an oscillation thus increasing the period of oscillations.

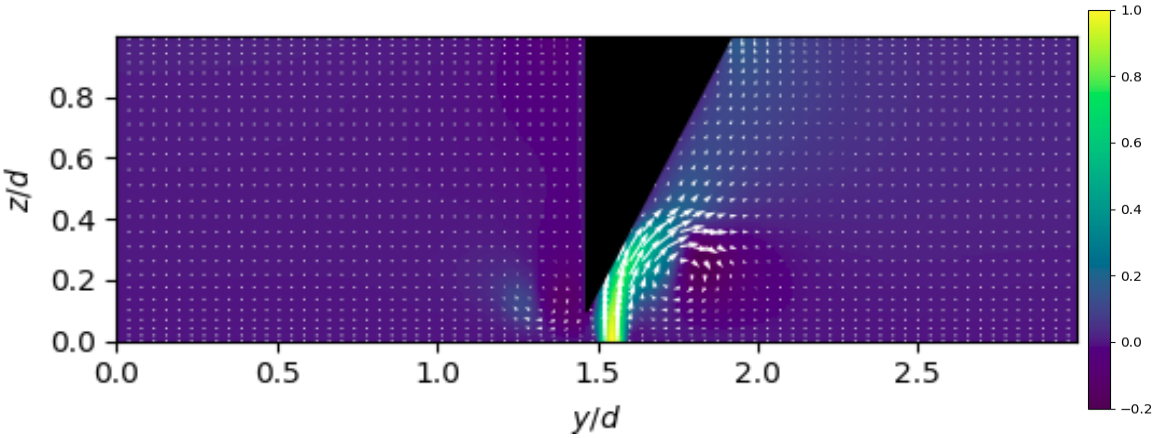

FIG 3. 23: CASE-III WITH H=0.036

The offset and its corresponding period of oscillation is recorded in the Table 3.5 and the trend is captured in the following figure. We see a positive correlation between the offset values with the period of oscillations. Increasing the offset from -0.1 to 0.036 physically means moving the jet from left side of the labium to the right. As the offset is increased, the distance for the jet to complete one oscillation also increases resulting in a greater period of oscillations with no oscillations at h=-0.1.

TABLE 3. 5: PERIOD OF OSCILLATIONS FOR DIFFERENT OFFSET VALUES

h	Period
-0.1	No oscillations
-0.038	0.74
0	0.85
0.036	0.95

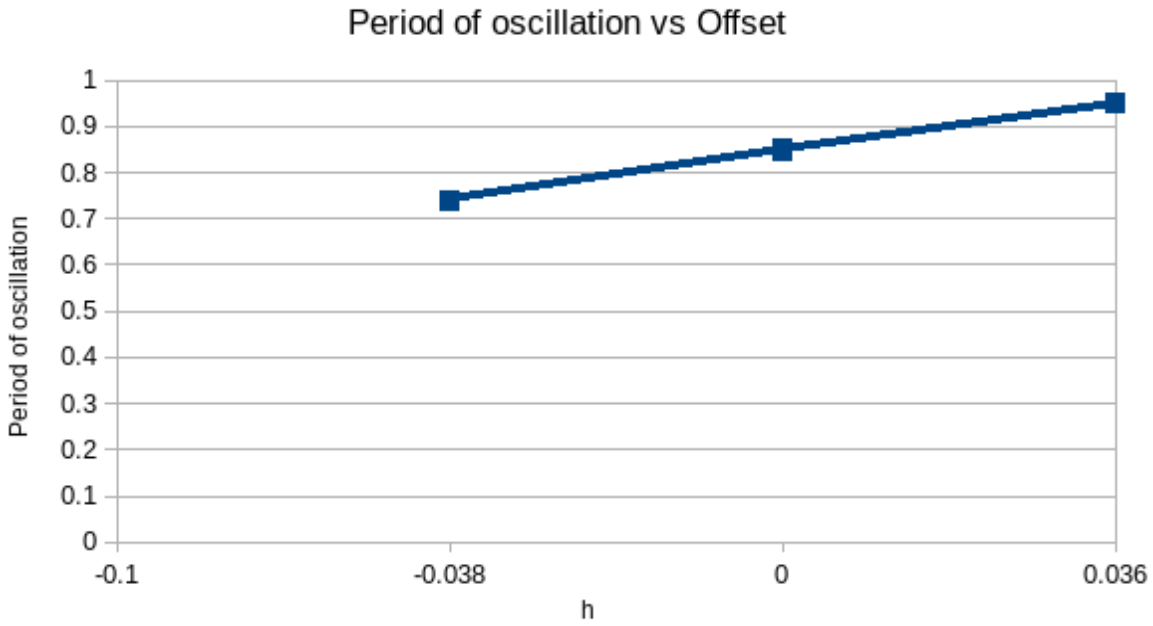

FIG 3. 24: PERIOD OF OSCILLATIONS FOR DIFFERENT VALUES OF OFFSET 'H'

3.6 Effect of outflow Courant number

An outflow Courant number is introduced in the wave equation at the last grid point. This condition is needed to evolve the velocity in such a way that

vorticity is allowed to exit the domain. In principle, the results should not depend on the Courant number, because it is a numerical parameter, and lacks physical meaning. We checked this by repeating the simulation for Reynolds number 1000 and jet width 0.1L for different outflow Courant numbers, i.e. 0.2, 0.4, and 0.8. There is no apparent change in the period of the oscillations, indicating that the simulation is robust to the outflow condition.

4. Conclusions

It has been shown that the flow on a flute labium can be effectively and reliably simulated using incompressible DNS. The oscillation period of a certain flow regime around the labium is well reproduced with DNS.

The jet is observed to have no oscillations at low Reynolds numbers, such as 500, for any labium angles in our investigation. The jet Reynolds number needs to exceed a certain Reynolds number threshold, over 500 in most cases, for the instabilities to rise enough to cause consistent oscillations around the flute labium. We have also observed that the parameters that make the period smaller for oscillations of the jet are labium sharpness and jet offset with respect to the labium. Making the labium sharper as well as moving the jet closer to the labium nozzle makes the oscillations more frequent and reduces the period. The farther away the jet is from the labium nozzle (sharp corner) and the bigger the angle of labium, the greater the oscillation period and hence, lower frequency of oscillation.

Unlike the parabolic profile with smoothened velocity coming out from the source, velocity for the uniform profile only smooths out as it travels away from the

source as the air particles outside the jet interact and become a part of the smoothing of the profile. Simultaneously, as the jet hits the labium it also experiences some obstruction in velocity due to viscous effects and velocity boundary layer develops along the labium surface downstream of the flow. The average velocities of the two different profiles are also different. These differences in interaction with the domain exhibited by the different velocity profiles of the jet significantly affect not only the oscillation period, but also the threshold Reynolds numbers at which the jet starts to oscillate.

The work presented here also opens up the possibilities of investigating the effects of several other parameters. These parameters could include changing the direction/orientation of the incident jet, shape of the flue exit, effects of other velocity profiles, and changing the distance between the flue exit and the labium etc. The investigations could be very useful for modeling the mouthpiece of flute instruments and could come in handy for a flautist or a flute maker. Modelling a complete recorder flute with a resonator, or other flute instruments like the organ pipe etc. requires even more work since the interaction of flow and its response from the resonator is still not understood. Nevertheless, having a tool that accurately simulated the flow response at the mouthpiece of such instruments is in itself of utmost value in flute research that trims down on trial and error in the art of flute designing and brings together experts in flute making and mathematical modeling under one roof.

References

[1] P. de la Cuadra, T. Smyth, C. Chafe, and H. Baoqiang. “Waveguide simulation of neolithic chinese flutes.” Proceedings of ISMA, *International Symposium on Musical Acoustics*, Perugia, Italy, 2001.

[2] B. Fabre. ”les bois.” notes from the course” journńées p´edagogiques physique des instruments de musique.” organized by sfa at enst paris. Available at: www.sfa.asso.fr, 2000.

[3] http://hyperphysics.phy-astr.gsu.edu/hbase/Music/edge.html

[4] D. Bernoulli. “Sur le son et sur les tons des tuyaux d’orgue differemment constru-its. Memoire.”, *Academie Royale des Sciences*, 1762.

[5] M. Mersenne. Harmonie Universelle. Facsimil edition from CNRS, 1636.

[6] H. Helmholtz. On the sensations of tone. Dover edition, NY, 1885.

[7] Lord Rayleigh. The Theory of Sound. Dover, reprint (1945), New-York, 1894.

[8] A. Powell. “On the edgetone.” *J. Acoust. Soc. Am., 33(4):395–409,* April 1961.

[9] N.H. Fletcher. “Air flow and sound generation in musical wind instruments.” *Ann. Rev. Fluid Mech., 11:123–146,* 1979.

[10] M.S. Howe. “Contribution to the theory of aerodynamic sound, with application to excess jet noise and the theory of the flute.” *J. Fluid Mech., 71:625–673,* 1975.

[11] Lee Miles. Playing the Native American flute. 2014

[12] J.W. Coltman. “Sounding mechanism of the flute and organ pipe.” *J. Acoust. Soc. Am., 44:983–992*, 1968.

[13] J.W. Coltman. “Jet drive mechanism in edge tones and organ pipes.” *J. Acoust. Soc. Am., 60(3):725–733*, September 1976.

[14] B. Fabre and A. Hirschberg. “Physical modeling of flue instruments: a review of lumped models.” *Acta Acustica, 86:599–610,* 2000.

[15] http://www.flute-a-bec.com/acoustiquegb.html

[16] S. Dequand. "Simplified models of flue instruments: Influence of mouth geometry on the sound source." *The Journal of the Acoustical Society of America 113*, 1724 (2003)

[17] M. P. Verge, R. Causse´, ,B. Fabre, A. Hirschberg, A.P.J. Wijnands, and A. van Steenbergen. "Jet Oscillations and Jet Drive in Recorderlike Instruments." *Acta Acustic. united with Acustica 2, 403–419.* 1994.

[18] B. Fabre, A. Hirschberg, and A.P.J. Wijnands. "Vortex shedding in steady oscillations of a flue organ pipe." *Acta Acustica, 82:811–823,* 1996.

[19] M. M. Rai, and P. Moin. "Direct simulations of turbulent flow using finite-difference schemes." *J. Comput. Phys.* 96, 15 1991.

[20] Choi, P. Moin, and J. Kim, *Ph.D. thesis TF-55*, Stanford University, 1992 (unpublished).

[21] E. A. Fadlun ,1 R. Verzicco, P. Orlandi, and J. Mohd-Yusof. "Combined Immersed-Boundary Finite-Difference Methods for Three-Dimensional Complex Flow Simulations"

[22] D. K. Holger, T.A Wilson, and G.S Beavers, "Fluid mechanics of the edge-tone." *J. Acoust. Soc. Am.* ***62***, *1116–1128*. (**1977**).

[23] J. Kim, and P. Moin. "Application of a fractional step method to incompressible Navier-Stokes Equations." *J. Comput. Phys. 59(2): 308-323,* June 1985.

[24] https://newt.phys.unsw.edu.au/jw/fluteacoustics.html

[25] Rayleigh, O. M, F. R. S. "The theory of the Helmholtz resonator." *Royal Society 92(638),* 1916

[26] B. Fabre. "La Production de Son dans les Instruments à Embouchure de Flûte: Modèle Aéro-Acoustique pour la Simulation Temporelle." PhD thesis, Universit´e du Maine, Le Mans, France, 1992.

[27] S.A. Elder. "On the mechanism of sound production in organ pipes." *J. Acoust. Soc. Am.*, *54:1554–1564,* 1973.

[28] D.G. Crighton. “The edgetone feedback cycle. Linear theory for the operating stages.” *J. Fluid Mech., 234:361–391,* 1992.

[29] D.W. Bechert. “Excitation of instability waves in free shear layers part 1: theory.” *J. Fluid Mech., 186:47–62*, 1988.

[30] L. Cremer and H. Ising. “Die selbsterregten Schwingungen von Orgelpfeifen.” *Acustica*, *19:143–153*, 1967–68.